ETH
Eidgenössische Technische Hochschule Zürich
Swiss Federal Institute of Technology Zurich

Seminar for Applied Mathematics SAM

Discontinuous Galerkin methods for acoustic wave propagation in polygons

F. Müller and D. Schötzau and Ch. Schwab

Research Report No. 2018-02
January 2018

Seminar für Angewandte Mathematik
Eidgenössische Technische Hochschule
CH-8092 Zürich
Switzerland

Funding SNF: 200021_149819/1
Funding: Natural Sciences and Engineering Research Council of Canada (NSERC)

DISCONTINUOUS GALERKIN METHODS FOR ACOUSTIC WAVE PROPAGATION IN POLYGONS

FABIAN MÜLLER, DOMINIK SCHÖTZAU, AND CHRISTOPH SCHWAB

ABSTRACT. We analyze space semi-discretization of linear, second-order wave equation by discontinuous Galerkin methods in two-dimensional polygonal domains where solutions exhibit singular behavior near corners. To resolve these singularities, we consider two families of locally refined meshes: graded meshes and bisection refinement meshes. We prove that for appropriately chosen refinement parameters, optimal asymptotic rates of convergence with respect to the total number of degrees of freedom are obtained, both in the energy norm errors and the $\mathcal{L}^2$-norm errors. The theoretical convergence orders are confirmed in a series of numerical experiments which also indicate that analogous results hold for incompatible data which is not covered by the currently available regularity theory.

1. INTRODUCTION

Linear, second-order hyperbolic partial differential equations (PDEs) play a crucial role in simulating wave propagation phenomena appearing in electromagnetics, elastodynamics or acoustics. To numerically approximate wave equations, we use the standard "method of lines" approach: the solution $u(\mathbf{x}, t)$ is viewed as a mapping from $t \in \overline{\mathsf{J}} = [0, \mathsf{T}]$ into a function space V over a spatial domain Ω (in our case a closed subspace of $H^1(\Omega)$). A Galerkin ansatz with a family of finite-dimensional subspaces of V leads to an ordinary differential equation (ODE) which can be numerically solved by means of suitable time-stepping methods.

However, even when using an explicit time-stepping scheme, each time-step requires the inversion of a mass-matrix. Therefore, it is desirable to use a spatial semi-discretization for which mass-matrices are easily invertible. One popular technique that yields block-diagonal mass-matrices for low-order continuous finite element methods (FEMs) in space is mass-lumping, see for example [8] and the references therein. An alternative approach is based on employing discontinuous Galerkin finite element methods (DGFEMs). By construction, these methods provide block-diagonal mass-matrices, which can be readily inverted in a block-by-block fashion.

Here, as in the works [13, 18, 16], we focus on symmetric interior penalty discontinuous Galerkin (SIPDG) finite element methods, which yield symmetric positive definite stiffness matrices in space (for symmetric elliptic spatial operators). Hence, SIPDG semi-discretizations conserve (a discrete version of) the energy for all times and are free of any (unnecessary) damping. In addition, SIPDG methods

Key words and phrases. Linear Wave Equations, Finite Element Methods, Discontinuous Galerkin Methods, Corner Singularities, Lipschitz Domains .

Research supported by the Swiss National Science Foundation under Grant No. SNF 200021_149819/1 and by the Natural Sciences and Engineering Research Council of Canada (NSERC). This paper benefitted from helpful discussions at the Mathematical Research Institute Oberwolfach (MFO) during meeting No.1711, March 13–17, 2017.

are adjoint-consistent in the sense of [2] and yield optimal order $\mathcal{L}^2$-norm errors in space. We point out that although we consider SIPDG methods in detail, our techniques are equally well and *mutatis mutandis* applicable to a much wider range of DG methods, for example, by employing the unifying framework of [2]. We refer to [33, 30] and the references therein for further details and developments on DG error analyses.

For elliptic PDEs in polygonal domains Ω, the values of the opening angles determine the Sobolev regularity of the solutions; see [20, 12, 6] (we also refer to [24] for polyhedral domains). Analogous regularity results for linear, second-order wave equations are due to [31, 19, 23] and more recently to [28]. There, the regularity of a wide class of boundary-transmission problems for second-order linear hyperbolic systems with piecewise constant coefficients was investigated in polygonal domains. The regularity results in [28, Section 2.6.2] are the basis of our convergence analysis.

A natural way to approximate singular solutions is to use local mesh refinement near corners of the domain. Here we consider the following two strategies: (i) graded mesh families as in [5] (we refer to [7, 1] for more recent variants, and to the LNG_FEM software package [22]), and (ii) bisection refinement meshes obtained by new newest vertex bisection (NVB) as in [11]. In [26, 27] and based on the regularity results in [31, 19, 23], it was shown that conforming finite element semi-discretizations of the wave equation on such mesh families indeed yield quasi-optimal convergence rates (with respect to the total number of degrees of freedom). For discontinuous and non-conforming Galerkin methods for wave equations, no such results seem to be available in the literature. For example, the analysis of [13] is based on uniform mesh families and on sufficient regularity of the underlying solutions. Similar assumptions have recently been made in [18, 16]. On the other hand, for linear elliptic PDEs in polygonal domains, SIPDG discretizations based on graded mesh families were investigated in the thesis [37], the results of which were then substantially extended in the recent work [25]. In particular, bisection refinement mesh families as in [11] were also included in the analysis there. Thus, the main goal of the present article is to extend the results of [13] to problems with singular solutions. Analogous to the elliptic case studied in [25], we show optimal error estimates for the DG energy norm and the $\mathcal{L}^2$-norm errors for the above-mentioned two families of locally refined meshes. These estimates are proved with the crucial help of the (elliptic) Galerkin projection, whose approximation properties were established in [25]. We present some numerical experiments to confirm the quasi-optimality of our error estimates on mesh sequences with local refinement.

The paper is structured as follows: In Section 2, we introduce polygonal domains, define our model wave equation and review the regularity of solutions in polygonal domains. In Sections 3 and 4, we recall the SIPDG method and state our main results (see Theorem 4.3). The proofs of these results are provided in Section 5. Finally, in Section 6, numerical tests are shown.

Throughout, we use standard notation. In particular, for a domain $G \subseteq \mathbb{R}^d$, $d \geq 1$, we write $\mathcal{C}_0^\infty(G)$ for the space of all smooth functions with compact support in G. For $q \in [1, \infty]$, the Lebesgue space of q-integrable functions is denoted by $\mathcal{L}^q(G)$. The standard inner product in $\mathcal{L}^2(G)$ or $\mathcal{L}^2(\Omega)^d$ is written as $(\cdot, \cdot)_G$ or simply as $(\cdot, \cdot)$ if G is clear from the context. For $k \in \mathbb{N}$, the classical Sobolev spaces of functions in $\mathcal{L}^q(G)$ with q-integrable derivatives of order up to k will

be denoted by $W^{k,q}(G)$, and by $H^k(G)$ if $q = 2$. For $J = (a, b)$ and a Sobolev space $X(G)$ in space, we denote by $\mathcal{C}^k(\overline{J}; X(G))$ and $\mathcal{L}^q(J; X(G))$ the spaces of all functions $J \to X(G)$ which are k-times continuously differentiable in $\overline{J}$ and q-integrable in J with values in $X(G)$, respectively.

2. Model problem

We define polygonal domains, introduce our model wave equation and review regularity results in weighted Sobolev spaces.

2.1. **Polygonal domains.** Let $\Omega \subseteq \mathbb{R}^2$ be an open, bounded two-dimensional domain with straight edges. Throughout, we assume Ω to be a polygonal domain i.e., its boundary $\partial\Omega$ can be written as the closure of a finite union of $\mathsf{M} \in \mathbb{N}$ open and straight line segments e_i of positive one-dimensional measure:

$$\partial\Omega = \bigcup_{i=1}^{\mathsf{M}} \overline{e}_i \,, \qquad \int_{e_i} dS > 0 \quad \forall\, i = 1, \dots \mathsf{M} \,. \tag{2.1}$$

The vertices of the polygon Ω are denoted by $\mathbf{c}_i := \overline{e}_i \cap \overline{e}_{i+1}$, $i = 1, \dots \mathsf{M}$, where the indices i are taken modulo M, i.e., we have $e_{\mathsf{M}+1} = e_1$. We assume the vertices to be numbered clockwise. We define the set of all vertices as $\mathcal{S} := \{\mathbf{c}_i \,:\, i = 1, \dots, \mathsf{M}\}$. For all i, the interior opening angle of the domain at $\mathbf{c}_i$ is measured in positive orientation and will be denoted by $\omega_i \in (0, 2\pi]$, $i = 1, \dots, \mathsf{M}$. The case $\omega_i = \pi$ is used to describe changing boundary conditions at $\mathbf{c}_i$ along the straight line segment $\overline{e}_i \cap \overline{e}_{i+1}$. The case $\omega_i = 2\pi$ corresponds to a slit (non Lipschitz) domain which is commonly used in fracture mechanics to model a cracked specimen.

At each vertex $\mathbf{c}_i$, we introduce local conical domains defined by

$$\Omega_i := \{\mathbf{x} \in \Omega \,:\, |\mathbf{x} - \mathbf{c}_i| < R_i\} \,, \qquad i = 1, \dots, \mathsf{M}, \tag{2.2}$$

where $0 < R_i < \frac{1}{2} \min_{j \neq i} |\mathbf{c}_i - \mathbf{c}_j|$. The cones Ω_i are mutually disjoint and $\partial\Omega_i \cap \partial\Omega \subset \overline{e}_i \cup \overline{e}_{i+1}$.

2.2. **Model wave equation.** Let Ω be a polygonal domain with straight edges. We write $\{1, \dots, \mathsf{M}\} = \mathcal{D} \cup \mathcal{N}$, where $\mathcal{D}$ and $\mathcal{N}$ denote the index sets of the edges e_i, on which Dirichlet and Neumann boundary conditions are applied, respectively. This leads to the partition $\partial\Omega = \overline{\Gamma}_D \cup \overline{\Gamma}_N$, where $\overline{\Gamma}_D = \cup_{i \in \mathcal{D}} \overline{e}_i$ and $\overline{\Gamma}_N = \cup_{i \in \mathcal{N}} \overline{e}_i$. In order to avoid technicalities associated with the pure Neumann case and to lighten the notation, we shall assume in the following that $\mathcal{D} \neq \emptyset$. We then introduce the energy space

$$V := \{\, v \in H^1(\Omega) \,:\, v|_{\Gamma_D} = 0 \,\} \,. \tag{2.3}$$

Then, let $0 < \mathsf{T} < \infty$ and $\mathsf{J} := (0, \mathsf{T})$. For given initial data $u^0 \in V$, $u^1 \in \mathcal{L}^2(\Omega)$, a given forcing term $f \in \mathcal{L}^2(\mathsf{J}; \mathcal{L}^2(\Omega))$ and a constant wave speed coefficient $\mathsf{c} > 0$, we introduce the model acoustic wave equation:

$$\partial_t^2 u - \nabla \cdot (\mathsf{c}\nabla u) = f \qquad \text{in } \Omega \times \mathsf{J}\,, \tag{2.4}$$

$$u = 0 \qquad \text{on } \Gamma_D \times \mathsf{J}\,, \tag{2.5}$$

$$\boldsymbol{\nu} \cdot (\mathsf{c}\nabla u) = 0 \qquad \text{on } \Gamma_N \times \mathsf{J}\,, \tag{2.6}$$

$$u(\cdot,0) = u^0 \qquad \text{in } \Omega\,, \tag{2.7}$$

$$\partial_t u(\cdot,0) = u^1 \qquad \text{in } \Omega\,, \tag{2.8}$$

where $\boldsymbol{\nu}$ is the outward pointing unit normal on the boundary $\partial\Omega$. Since c is a constant, by rescaling we could assume without loss of generality that $\mathsf{c} = 1$.

We consider a standard weak form of (2.4)–(2.8), which is pointwise in time and variationally in space. It reads as follows: Find $u \in \mathcal{C}^0(\overline{\mathsf{J}}; V)$ with $\partial_t u \in \mathcal{C}^0(\overline{\mathsf{J}}; \mathcal{L}^2(\Omega))$ such that $u(\cdot,0) = u^0$ in V, $\partial_t u(\cdot,0) = u^1$ in $\mathcal{L}^2(\Omega)$ and

$$\langle \partial_t^2 u(\cdot,t), v\rangle_{V^*,V} + a(u(\cdot,t), v) = (f(\cdot,t), v)\,, \tag{2.9}$$

for all $t \in \mathsf{J}$ and $v \in V$, where the Galerkin form $a(w,v)$ on $V \times V$ is given by

$$a(w,v) := \int_\Omega \mathsf{c}\nabla w \cdot \nabla v \, d\mathbf{x}\,. \tag{2.10}$$

Problem (2.9)– (2.10) is a special case of the class of problems called "Problème P_2" in [9]. Therefore, we deduce from [9, Chpt. XVIII.5, Thms. 3 and 4] the existence and uniqueness of weak solutions u, as well as the stability estimate

$$\begin{aligned} \|u\|_{\mathcal{C}^0(\overline{\mathsf{J}};V)} + \|\partial_t u\|_{\mathcal{C}^0(\overline{\mathsf{J}};\mathcal{L}^2(\Omega))} + \|\partial_t^2 u\|_{\mathcal{C}^0(\overline{\mathsf{J}};V^\star)} \\ \le C\big(\|f\|_{\mathcal{L}^2(\mathsf{J};\mathcal{L}^2(\Omega))} + \|u^0\|_V + \|u^1\|_{\mathcal{L}^2(\Omega)}\big)\,, \end{aligned} \tag{2.11}$$

with V^* denoting the dual space of V, and with a constant $C > 0$ depending on Ω, T, $\mathcal{D}$, $\mathcal{N}$ and on the coefficient c. Moreover, if $u^0, u^1 \in \mathcal{C}_0^\infty(\Omega)$ and $f \in \mathcal{C}_0^\infty(\Omega \times \mathsf{J})$, we have for all $s \in \mathbb{N}_0$ that

$$u \in \mathcal{C}^{s+2}(\overline{\mathsf{J}}; V^\star) \cap \mathcal{C}^{s+1}(\overline{\mathsf{J}}; \mathcal{L}^2(\Omega)) \cap \mathcal{C}^s(\overline{\mathsf{J}}; V))\,; \tag{2.12}$$

see, e.g., [38, Thm 30.1]. This property can also be seen by expanding the solutions into eigenfunctions using separation of variables.

2.3. **Weighted Sobolev spaces.** To each vertex $\mathbf{c}_i$ of Ω, we assign a *weight exponent* $\delta_i \in [0,1)$. The entries δ_i are collected in the *weight exponent vector* $\boldsymbol{\delta} = \{\delta_i\}_{i=1}^{\mathsf{M}} \in [0,1)^{\mathsf{M}}$. For $\xi \in \mathbb{R}$, we introduce the notation $\boldsymbol{\delta} + \xi := \{\delta_i + \xi\}_{i=1}^{\mathsf{M}}$. Similarly, inequalities of the form $\boldsymbol{\delta} < \xi$ are understood componentwise.

Next, we introduce the *weight function*:

$$\Phi_{\boldsymbol{\delta}}(\mathbf{x}) := \prod_{i=1}^{\mathsf{M}} r_i(\mathbf{x})^{\delta_i}\,. \tag{2.13}$$

where $r_i(\mathbf{x}) = |\mathbf{x} - \mathbf{c}_i|$. Given integers $k \ge \ell \ge 0$, we define the weighted Sobolev spaces $H^{k,\ell}_{\boldsymbol{\delta}}(\Omega)$ as the completion of $\mathcal{C}^\infty(\overline{\Omega})$ with respect to the norm

$$\|w\|^2_{H^{k,\ell}_{\boldsymbol{\delta}}(\Omega)} := \begin{cases} |w|^2_{H^{k,0}_{\boldsymbol{\delta}}(\Omega)}, & \ell = 0, \\ \|w\|^2_{H^{\ell-1}(\Omega)} + |w|^2_{H^{k,\ell}_{\boldsymbol{\delta}}(\Omega)}, & \ell \ge 1. \end{cases} \tag{2.14}$$

Here, the semi-norm $|w|_{H^{k,\ell}_{\boldsymbol{\delta}}(\Omega)}$ is given by

$$|w|^2_{H^{s,\ell}_{\boldsymbol{\delta}}(\Omega)} := \sum_{m=\ell}^{k} \|\Phi_{\boldsymbol{\delta}+m-\ell}\,|\mathsf{D}^m w|\|^2_{\mathcal{L}^2(\Omega)}\,, \tag{2.15}$$

and $|\mathsf{D}^m w|^2 := \sum_{|\boldsymbol{\alpha}|=m} |\mathsf{D}^{\boldsymbol{\alpha}} w|^2$, with $\mathsf{D}^{\boldsymbol{\alpha}} w$ denoting the partial derivative of w with respect to the multi-index $\boldsymbol{\alpha} \in \mathbb{N}_0^2$.

We shall also make use of the weighted spaces $H^{k,l}_{\delta_i}(\Omega)$, their associated norms $\|w\|_{H^{k,l}_{\delta_i}(\Omega)}$ and semi-norms $|w|_{H^{k,l}_{\delta_i}(\Omega)}$, which are defined completely analogously, but with respect to the weight $r_i(\mathbf{x})^{\delta_i}$. Furthermore, over subdomains $\Omega' \subseteq \Omega$ the weighted spaces and norms are defined by replacing the domains of integration by Ω'.

We recall the following properties; see [25, Lem. 2.3] and the references there.

Lemma 2.1. *Let $\boldsymbol{\delta} \in [0,1)^{\mathsf{M}}$. There holds:*

(i) *We have the continuous embeddings*

$$H^{k,2}_{\boldsymbol{\delta}}(\Omega) \hookrightarrow H^{2,2}_{\boldsymbol{\delta}}(\Omega) \hookrightarrow \mathcal{C}^0(\overline{\Omega})\,, \qquad k \geq 2. \tag{2.16}$$

(ii) *For $k \geq \ell \geq 1$, let $w \in H^{k,\ell}_{\boldsymbol{\delta}}(\Omega)$ and let $\boldsymbol{\alpha} \in \mathbb{N}_0^2$ be such that $|\boldsymbol{\alpha}| \leq \ell$. Then, we have $\mathsf{D}^{\boldsymbol{\alpha}} w \in H^{k-|\boldsymbol{\alpha}|,\ell-|\boldsymbol{\alpha}|}_{\boldsymbol{\delta}}(\Omega)$ and*

$$\|\mathsf{D}^{\boldsymbol{\alpha}} w\|_{H^{k-|\boldsymbol{\alpha}|,\ell-|\boldsymbol{\alpha}|}_{\boldsymbol{\delta}}(\Omega)} \leq \|w\|_{H^{k,\ell}_{\boldsymbol{\delta}}(\Omega)}. \tag{2.17}$$

(iii) *Let $f \in H^{0,0}_{\boldsymbol{\delta}}(\Omega)$. Then $\int_\Omega f v\,d\mathbf{x}$ is a linear continuous functional on $H^1(\Omega)$ and*

$$\Big|\int_\Omega f v\,d\mathbf{x}\Big| \leq C\|f\|_{H^{0,0}_{\boldsymbol{\delta}}(\Omega)}\|v\|_{H^1(\Omega)}, \qquad v \in H^1(\Omega), \tag{2.18}$$

with a constant $C > 0$ depending on $\boldsymbol{\delta}$.

2.4. **Regularity in weighted spaces.** In polygonal domains, solutions to problem (2.4)–(2.8) typically have low regularity due to the appearance of singular solution components near corners. Sharp regularity estimates in two dimensions are now available in scales of weighted Sobolev spaces, including solution asymptotics towards corners $\mathbf{c}_i \in \mathcal{S}$. These results are due to [31, 19, 23] and, in the particular form required here, to [28] and to [26, 27]. Specifically, in [28, Cor. 2.6.6], regularity results for solutions u of wave equations with $\mathcal{C}^s$-regularity with respect to the time variable, taking values in $H^{k+1,2}_{\boldsymbol{\delta}}(\Omega)$ were proved for boundary-transmission problems for linear second-order hyperbolic systems with piecewise constant coefficients on polygons, of which the wave equation (2.4)-(2.8) is a particular case. This regularity result will be the basis of our analysis.

Proposition 2.2. *For smooth data $u^0, u^1 \in \mathcal{C}^\infty_0(\Omega)$ and for $f \in \mathcal{C}^\infty_0(\Omega \times \mathsf{J})$, let u be the weak solution of (2.4)–(2.8) in the sense of (2.9). Then, there exists $\boldsymbol{\delta} = \{\delta_i\}_{i=1}^{\mathsf{M}} \in [0,1)^{\mathsf{M}}$ such that for all $s \in \mathbb{N}_0$ and $k \in \mathbb{N}$,*

$$u \in \mathcal{C}^s(\overline{\mathsf{J}}; H^{k+1,2}_{\boldsymbol{\delta}}(\Omega))\,. \tag{2.19}$$

Remark 2.3. *The weights $\boldsymbol{\delta} = \{\delta_i\}_{i=1}^{\mathsf{M}}$ in Proposition 2.2 are chosen according to $\delta_i > \delta_i^*$, $i = 1, \ldots, \mathsf{M}$, with the lower bounds δ_i^* defined as follows: There exists a singular exponent $\lambda_i > 0$ such that*

$$\delta_i^* := \max(0, 1 - \lambda_i), \qquad i = 1, \ldots, \mathsf{M}\,, \tag{2.20}$$

where λ_i depends on Ω, $\mathcal{D}$, $\mathcal{N}$ and, in general, on the elliptic part of the spatial operator in (2.4)*. Note that the conditions*

$$\max(0, \delta_i^*) < \delta_i < 1, \qquad i = 1, \dots, \mathsf{M} \tag{2.21}$$

correspond to the range of the elliptic regularity shifts of [5, 4, 3] *in the scale of corner-weighted spaces $H^{k,\ell}_{\boldsymbol{\delta}}(\Omega)$, which arises naturally in the study of polygonal corner singularities for linear, elliptic problems. More precisely, for weight exponents δ_i satisfying* (2.21)*, the weak solution $z \in V$ of the elliptic problem*

$$-\nabla \cdot (\mathsf{c}\nabla z) = g \qquad \text{in } \Omega\,, \tag{2.22}$$

$$z = 0 \qquad \text{on } \Gamma_D\,, \tag{2.23}$$

$$\boldsymbol{\nu} \cdot (\mathsf{c}\nabla z) = 0 \qquad \text{on } \Gamma_N\,, \tag{2.24}$$

satisfies the following elliptic regularity property: for $k \geq 1$ and $g \in H^{k-1,0}_{\boldsymbol{\delta}}(\Omega)$, we have $z \in H^{k+1,2}_{\boldsymbol{\delta}}(\Omega)$ and

$$\|z\|_{H^{k+1,2}_{\boldsymbol{\delta}}(\Omega)} \leq C_{stab,k} \|g\|_{H^{k-1,0}_{\boldsymbol{\delta}}(\Omega)}\,, \tag{2.25}$$

for a constant $C_{stab,k} > 0$ depending on the order k, the domain Ω, the sets $\mathcal{D}, \mathcal{N}$, and the coefficient c. In fact, if the coefficient $\mathsf{c} > 0$ is constant in (2.4)– (2.8)*, we have*

$$\lambda_i = \begin{cases} \pi/\omega_i & \text{if } \{i, i+1\} \in \mathcal{D} \text{ or } \{i, i+1\} \in \mathcal{N}, \\ \pi/(2\omega_i) & \text{otherwise}\,; \end{cases} \tag{2.26}$$

see [21, Chpt. 2.1].

3. Discontinuous Galerkin Discretization

We introduce discontinous finite element spaces and review the symmetric interior penalty DG method for the spatial approximation of (2.4)–(2.8).

3.1. **Meshes, edges and trace operators.** Let $\mathcal{T}$ be a partition of Ω into straight-sided triangles K. For ease of presentation, we restrict ourselves to regular triangulations and comment on extensions to irregular meshes in Section 7. The triangulations are supposed to be sufficiently fine so that each element K contains at most one vertex $\mathbf{c}_i$. For $K \in \mathcal{T}$, we denote by $\mathcal{P}^p(K)$ the polynomials on K of total degree at most p. The diameter of $K \in \mathcal{T}$ is denoted by h_K and is referred to as the elemental mesh size of K. Furthermore, we denote by ρ_K inradius of K. The mesh-width of $\mathcal{T}$ is given by $h = h(\mathcal{T}) := \max_{K\in\mathcal{T}} h_K$. We assume the triangulations to be shape-regular: there exists a constant $\kappa > 0$ such that

$$\rho_K \leq h_K \leq \kappa \rho_K, \qquad \forall\, K \in \mathcal{T}\,, \tag{3.1}$$

uniformly in the mesh sequence.

Edges are defined as follows: If K and K' are adjacent elements of the triangulation $\mathcal{T}$ with $\int_{\partial K \cap \partial K'} dS > 0$, we call the intersection $e = \partial K \cap \partial K'$ an interior edge. Elemental edges of K are supposed to lie at most on one boundary segment e_i, and if $\int_{\partial K \cap e_i} dS > 0$, we call the intersection $e = \partial K \cap e_i$ a boundary edge; it belongs to either Γ_D or Γ_N. Accordingly, we distinguish between Dirichlet and Neumann edges. The set of interior edges of a triangulation $\mathcal{T}$ is denoted by $\mathcal{E}_\mathcal{T}^\circ$, the set of Dirichlet boundary edges by $\mathcal{E}_\mathcal{T}^\mathcal{D}$, and the set of Neumann boundary edges by $\mathcal{E}_\mathcal{T}^\mathcal{N}$. Moreover, we define $\mathcal{E}_\mathcal{T} := \mathcal{E}_\mathcal{T}^\circ \cup \mathcal{E}_\mathcal{T}^\mathcal{D} \cup \mathcal{E}_\mathcal{T}^\mathcal{N}$. For $e \in \mathcal{E}_\mathcal{T}$, we denote by $\mathcal{P}^p(e)$ the

polynomials of degree at most p on e, and by h_e the length of e is denoted by h_e. With the shape-regularity assumption (3.1), it can be readily verified that

$$\kappa h_K \le h_e \le h_K, \tag{3.2}$$

for all $e \subset K$ with $e \in \mathcal{E}_\mathcal{T}$ and $K \in \mathcal{T}$.

We next define the usual trace operators. Let $K^+, K^- \in \mathcal{T}$ be two adjacent elements which share the interior edge $e = \partial K \cap \partial K' \in \mathcal{E}_\mathcal{T}^\circ$. We denote by $\boldsymbol{\nu}^\pm$ the outward pointing unit normals on $\partial K^\pm$. For a sufficiently smooth scalar function w or vector field $\mathbf{q}$, we denote the traces of w and $\mathbf{q}$ on e taken from within $K^\pm$ by $w^\pm$ and $\mathbf{q}^\pm$, respectively. We then define the jumps and the averages of w and $\mathbf{q}$ along e by

$$[\![w]\!] := w^+\boldsymbol{\nu}^+ + w^-\boldsymbol{\nu}^- \,, \qquad \langle\!\langle v \rangle\!\rangle := \frac{1}{2}(w^+ + w^-) \,, \tag{3.3}$$

$$[\![\mathbf{q}]\!] := \mathbf{q}^+ \cdot \boldsymbol{\nu}^+ + \mathbf{q}^- \cdot \boldsymbol{\nu}^- \,, \qquad \langle\!\langle \mathbf{q} \rangle\!\rangle := \frac{1}{2}(\mathbf{q}^+ + \mathbf{q}^-) \,. \tag{3.4}$$

If $e \in \mathcal{E}_\mathcal{T}^\mathcal{D}$ is a Dirichlet boundary edge, we set similarly $[\![w]\!] := w|_e\boldsymbol{\nu}$, $[\![\mathbf{q}]\!] = \mathbf{q}|_e \cdot \boldsymbol{\nu}$, as well as $\langle\!\langle w \rangle\!\rangle := w|_e$, $\langle\!\langle \mathbf{q} \rangle\!\rangle := \mathbf{q}|_e$.

3.2. **Corner elements.** For a mesh $\mathcal{T}$ on Ω, we introduce the set $\mathcal{K}^i(\mathcal{T})$ of corner elements of $\mathcal{T}$ abutting at corner $\mathbf{c}_i$

$$\mathcal{K}^i(\mathcal{T}) := \{ K \in \mathcal{T} \,:\, \overline{K} \cap \mathbf{c}_i \neq \emptyset \} \,. \tag{3.5}$$

Without loss of generality, we will assume that $\mathcal{K}^i(\mathcal{T}) \cap \mathcal{K}^j(\mathcal{T}) = \emptyset$ for $i \neq j$ and that $K \in \mathcal{K}^i(\mathcal{T})$ is located in the cone Ω_i (i.e., $\overline{K} \subset \Omega_i$). We then set

$$\mathcal{K}(\mathcal{T}) := \bigcup_{i=1}^{\mathsf{M}} \mathcal{K}^i(\mathcal{T}). \tag{3.6}$$

The following properties are from [37, Lems. 1.3.2 and 1.3.4]; see also [25, Lem. 5.2].

Lemma 3.1. *Let $K \in \mathcal{K}^i(\mathcal{T})$ be a corner element at corner $\mathbf{c}_i$ and $\delta_i \in [0,1)$ a weight exponent. Then:*

(i) $H^{0,0}_{\delta_i}(K) \subset \mathcal{L}^1(K)$ *and* $\|w\|_{\mathcal{L}^1(K)} \lesssim h_K^{1-\delta_i} |w|_{H^{0,0}_{\delta_i}(K)}$ *for* $w \in H^{0,0}_{\delta_i}(K)$.

(ii) $|\int_K wv\, d\mathbf{x}| \lesssim h_K^{1-\delta_i} |w|_{H^{0,0}_{\delta_i}(K)} \|v\|_{\mathcal{L}^\infty(K)}$ *for* $w \in H^{0,0}_{\delta_i}(K)$ *and* $v \in \mathcal{L}^\infty(K)$.

(iii) $\|w\|_{\mathcal{L}^1(\partial K)} \lesssim \|w\|_{\mathcal{L}^2(K)} + h_K^{1-\delta_i} |w|_{H^{1,1}_{\delta_i}(K)}$ *for* $w \in H^{1,1}_{\delta_i}(K)$.

(iv) $[\![w]\!]|_e = \mathbf{0}$ *in* $\mathcal{L}^1(e)^2$ *for* $w \in H^{1,1}_{\delta_i}(K)$ *and* $e \in \mathcal{E}_\mathcal{T}^\circ$ *with* $\overline{e} \cap \mathbf{c}_i \neq \emptyset$.

3.3. **Discretization in space.** For an approximation order $p \in \mathbb{N}$ and a given triangulation $\mathcal{T}$ of Ω, we introduce the discontinuous finite element space

$$V_p(\mathcal{T}) := \{ v \in \mathcal{L}^2(\Omega) \,:\, v|_K \in \mathcal{P}^p(K),\ K \in \mathcal{T} \} \,, \tag{3.7}$$

Remark 3.2. *The dimension $N(p,\mathcal{T}) := \dim(V_p(\mathcal{T}))$ is finite and convergence is usually achieved if $N \to \infty$. Here, we are interested in h-version SIPDG methods, where convergence is obtained by letting $h \to 0$ at a fixed, typically low polynomial order p. If clear from the context, we write N in place $N(p,\mathcal{T})$.*

Let $u_N^0, u_N^1 \in V_p(\mathcal{T})$ be discrete approximations to the initial data $u^0 \in V$, $u^1 \in \mathcal{L}^2(\Omega)$. The SIPDG semi-discretization of (2.9) reads as follows: find $u_N \in \mathcal{C}^2(\overline{\mathsf{J}}; V_p(\mathcal{T}))$ such that $u_N(\cdot,0) = u_N^0$, $\partial_t u_N(\cdot,0) = u_N^1$ and

$$(\partial_t^2 u_N(\cdot,t), v_N) + a_{DG}(u_N(\cdot,t), v_N) = \sum_{K\in\mathcal{T}} (f(\cdot,t), v_N)_K, \tag{3.8}$$

for all $t \in \mathsf{J}$ and $v_N \in V_p(\mathcal{T})$. Here, $a_{DG}(\cdot,\cdot)$ is the symmetric interior penalty bilinear form defined for $v, w \in V_p(\mathcal{T})$ by

$$\begin{aligned} a_{DG}(w,v) := &\sum_{K\in\mathcal{T}} \int_K \mathtt{c}\nabla w \cdot \nabla v \, d\mathbf{x} - \sum_{e\in\mathcal{E}_\mathcal{T}^\circ\cup\mathcal{E}_\mathcal{T}^\mathcal{D}} \int_e [\![v]\!] \cdot \langle\!\langle \mathtt{c}\nabla w \rangle\!\rangle \, dS \\ &- \sum_{e\in\mathcal{E}_\mathcal{T}^\circ\cup\mathcal{E}_\mathcal{T}^\mathcal{D}} \int_e [\![w]\!] \cdot \langle\!\langle \mathtt{c}\nabla v \rangle\!\rangle \, dS + \sum_{e\in\mathcal{E}_\mathcal{T}^\circ\cup\mathcal{E}_\mathcal{T}^\mathcal{D}} \int_e \mathtt{a}_\mathtt{e} [\![\mathtt{w}]\!] \cdot [\![\mathtt{v}]\!] \, \mathtt{dS} \, . \end{aligned} \tag{3.9}$$

The interior penalty function $\mathtt{a}$ in (3.9) is defined edgewise as

$$\mathtt{a}_\mathtt{e} := \mathtt{j}\,\mathtt{ch}_\mathtt{e}^{-1} \, , \qquad \mathtt{e} \in \mathcal{E}_\mathcal{T}^\circ \cup \mathcal{E}_\mathcal{T}^\mathcal{D} \, , \tag{3.10}$$

where $\mathtt{c} > 0$ is the (constant) coefficient in (2.4), $\mathtt{j} > 0$ is a sufficiently large constant as specified in Lemma 3.4 ahead, and where we recall that h_e denotes the length of edge e.

Remark 3.3. *For $f \in H_{\boldsymbol{\delta}}^{0,0}(\Omega)$ and $v_N \in V_p(\mathcal{T})$, the integrals $(f, v_N)_K$ in the right-hand side of* (3.8) *are well-defined for all $K \in \mathcal{T}$. In particular, for corner elements $K \in \mathcal{K}^i(\mathcal{T})$ at $\mathbf{c}_i$, these integrals are to be understood as bounded and bilinear forms in $\mathcal{L}^1(K) \times \mathcal{L}^\infty(K)$. This follows from the properties in Lemma 3.1 below.*

Upon introducing a basis of the FE space $V_p(\mathcal{T})$, the semi-discrete problem (3.8) yields a system of linear, second-order ordinary differential equations in time, which we assume here to be solved exactly. An error analysis for a fully discrete DG scheme, for sufficiently smooth solutions, was presented in [14]; an extension to the present framework will be presented elsewhere.

We further recall the discrete stability of the DG form $a_{DG}(\cdot,\cdot)$ over the FE space $V_p(\mathcal{T})$ with respect to the "DG energy norm" $|\!|\!| \cdot |\!|\!|_{DG}$ defined for $v \in V_p(\mathcal{T})$ by

$$|\!|\!| v |\!|\!|_{DG}^2 := \sum_{K\in\mathcal{T}} \left\| \mathtt{c}^{1/2}\nabla v \right\|_{\mathcal{L}^2(K)}^2 + J(v), \qquad J(v) := \sum_{e\in\mathcal{E}_\mathcal{T}^\circ\cup\mathcal{E}_\mathcal{T}^\mathcal{D}} \left\| \mathtt{a}_\mathtt{e}^{1/2} [\![\mathtt{v}]\!] \right\|_{\mathcal{L}^2(e)}^2 \, . \tag{3.11}$$

Here, the constants $\mathtt{j}$ in the definition (3.10) of $\mathtt{a}_\mathtt{e}$ are assumed bounded from below by a sufficiently large, positive constant $\mathtt{j}_* > 0$ as specified next.

Lemma 3.4. *There is $\mathtt{j}_* > 0$ only depending on κ in* (3.1) *and on the polynomial degree $p \geq 1$ such that for all $\mathtt{j} > \mathtt{j}_*$ in* (3.10) *there holds*

$$a_{DG}(v_N, v_N) \geq C_{coer} |\!|\!| v_N |\!|\!|_{DG}^2, \qquad v_N \in V_p(\mathcal{T}), \tag{3.12}$$

$$|a_{DG}(w_N, v_N)| \leq C_{cont} |\!|\!| w_N |\!|\!|_{DG} |\!|\!| v_N |\!|\!|_{DG}, \qquad v_N, w_N \in V_p(\mathcal{T}) \, , \tag{3.13}$$

with constants $C_{coer} > 0$ and $C_{cont} > 0$ independent of the elemental mesh sizes.

4. Main Results

Our goal is now to prove that for singular solutions in polygonal domains, optimal convergence rates in terms of N can be obtained on meshes with suitable refinement towards the vertices of the polygon Ω, analogous to what is well-known in conforming adaptive FEMs for elliptic problems; cf. [29] and the references therein. To this end, we introduce two types of mesh families with local refinement towards corners: *graded* mesh families and *bisection refinement* meshes. Our main results are stated in Theorem 4.3. They show that optimal asymptotic convergence rates can be recovered on the two locally refined mesh families, subject to sufficiently strong mesh refinement towards the singular points.

4.1. Graded mesh families.

We first recall the definition of graded mesh families as introduced in [5]. Recall further rom (3.6) that $\mathcal{K}(\mathcal{T})$ denotes the set of all elements abutting at corners.

Definition 4.1. *A family of triangulations $\mathcal{T}_{\boldsymbol{\beta}}$ is called graded towards the vertices in $\mathcal{S}$ with grading vector $\boldsymbol{\beta} = (\beta_1, \ldots, \beta_{\mathsf{M}})$, if there exists a uniform constant $C_{gr} > 0$ such that for all elements $K \in \mathcal{T}_{\boldsymbol{\beta}}$ in each triangulation one of the following conditions holds:*

(i) *If $K \in \mathcal{T}_{\boldsymbol{\beta}} \setminus \mathcal{K}(\mathcal{T}_{\boldsymbol{\beta}})$, then $C_{gr}^{-1} h \Phi_{\boldsymbol{\beta}}(\mathbf{x}) \leq h_K \leq C_{gr} h \Phi_{\boldsymbol{\beta}}(\mathbf{x})$ for all $\mathbf{x} \in K$.*
(ii) *If $K \in \mathcal{K}(\mathcal{T}_{\boldsymbol{\beta}})$, then $C_{gr}^{-1} \sup_{\mathbf{x}\in K} \Phi_{\boldsymbol{\beta}}(\mathbf{x}) \leq h_K \leq C_{gr} h \sup_{\mathbf{x}\in K} \Phi_{\boldsymbol{\beta}}(\mathbf{x})$.*

In [37] and [25], it was shown that DG methods for elliptic problems on graded mesh families converge optimally with respect to N, both in the DG energy norm and in the $\mathcal{L}^2$-norm. Other examples of graded mesh families and their constructions are well-known by now. We refer to [7] and to [22] for the software package LNG_FEM.

4.2. Bisection refinement meshes.

Alternatively, we consider meshes generated by the bisection refinement algorithm in [11, Pg. 926]. Its outline is as follows: Given an initial regular triangulation $\mathcal{T}_0$, the algorithm there takes as input parameters a granularity parameter h, a weight parameter $\gamma > 0$ and the number L of refinements (towards $\mathcal{S}$). In a first loop, it ensures that all elemental mesh sizes h_K are smaller than h. In a second loop, it refines $2L+1$ times towards corners using newest vertex bisection, where L is selected in dependence of h, p and the weight parameter γ as in (4.2) ahead. This results in a regular mesh denoted by $\mathcal{T}_{h,2(L+1)}$. We emphasize that the bisection refinement meshes constructed from the regular, simplicial initial mesh $\mathcal{T}_0$ gives rise to a shape-regular mesh family, where the condition (3.1) is satisfied with a constant κ depending on $\mathcal{T}_0$; see [11, Rem. 4.3, item (iv)].

For conforming finite element methods, it has been shown in [11, Thms 5.1 through 5.3] that the bisection refinement algorithm based on choosing suitable parameters captures solutions of elliptic problems that allow decompositions into regular parts and corner singularities at optimal convergence orders in N. In [25, Sect. 5.7], this result was generalized to the SIPDG framework and to functions in the weighted spaces $H^{k+1,2}_{\boldsymbol{\delta}}(\Omega)$.

4.3. Optimal error estimates.

We first introduce the notion of a locally refined mesh.

Definition 4.2. *Let $p \geq 1$ and $\boldsymbol{\delta} \in [0,1)^{\mathsf{M}}$ be a weight exponent vector. We call a a family of triangulations $\mathcal{T}$ of Ω* locally refined towards $\mathcal{S}$ with respect to $\boldsymbol{\delta}$ and p *if it is either*

(i) *a graded mesh family of meshes $\mathcal{T}_{\boldsymbol{\beta}}$ as in Definition 4.1, with grading parameters $\beta_i \in [\beta_i^*, 1)$, where*

$$\beta_i^* := 1 - \frac{1-\delta_i}{p}\,, \qquad i = 1, \ldots, \mathsf{M}. \tag{4.1}$$

(ii) *or a family of bisection refinement meshes $\mathcal{T}_{h,2(L+1)}$ as in* [11, Pg. 926]*, obtained by newest vertex bisection with parameters h, $\gamma \in (0, \gamma^*]$ and L satisfying*

$$\gamma^* := 1 - \max_{i=1}^{\mathsf{M}} \delta_i > 0 \quad \textit{and} \quad h \in [2^{-(L+1)\gamma/(p+1)}, 2^{-L\gamma/(p+1)}); \tag{4.2}$$

see [11, Eqn. (4.1) with $d = 2$].

Then, to state our a-priori error bounds, we follow [2] and introduce the ("lifted") space

$$\mathcal{V}_p(\mathcal{T}) := V + V_p(\mathcal{T})\,, \tag{4.3}$$

with the energy space V in (2.3). The space $\mathcal{V}_p(\mathcal{T})$ is equipped with the energy norm $|\!|\!| \cdot |\!|\!|_{DG}$ in (3.11), which is a norm for $\mathcal{D} \neq \emptyset$. In the pure Neumann case ($\mathcal{D} = \emptyset$), the map $w \mapsto |\!|\!| w |\!|\!|_{DG}$ is a semi-norm, which is zero if and only if w is constant. We further introduce the space $\mathcal{L}^\infty(\mathsf{J}; \mathcal{V}_p(\mathcal{T}))$ and equip it with the supremum norm

$$\|w\|_{\mathcal{L}^\infty(\mathsf{J};\mathcal{V}_p(\mathcal{T}))} := \sup_{t \in \mathsf{J}} |\!|\!| w(t) |\!|\!|_{DG}\,. \tag{4.4}$$

The discrete initial data u_N^0, u_N^1 in (3.8) are chosen as:

$$u_N^0 = \Pi_p u^0, \qquad u_N^1 = \Pi_p u^1, \tag{4.5}$$

where we denote by $\Pi_p : \mathcal{L}^2(\Omega) \to V_p(\mathcal{T})$ the $\mathcal{L}^2$-projection.

We now state our main results: optimal $\mathcal{L}^\infty(\mathsf{J}; \mathcal{V}_p(\mathcal{T}))$-norm and $\mathcal{L}^\infty(\mathsf{J}; \mathcal{L}^2(\Omega))$-norm error estimates (in space) on locally refined meshes.

Theorem 4.3. *Let $p \geq 1$ and $\boldsymbol{\delta} \in [0,1)^{\mathsf{M}}$ be as in* (2.21)*. For $1 \leq k \leq p$, let the solution u of the wave equation* (2.4)–(2.8) *satisfy*

$$u \in \mathcal{C}^2(\overline{\mathsf{J}}; H^{k+1,2}_{\boldsymbol{\delta}}(\Omega))\,; \tag{4.6}$$

Let $\mathcal{T}$ be a mesh (family) which is locally refined to $\mathcal{S}$ with respect to $\boldsymbol{\delta}$ and p as in Definition 4.2. Let u_N be the SIPDG approximation obtained in (3.8) *with $\mathsf{j} > \mathsf{j}_*$ and with the discrete initial data $u_N^0, u_N^1 \in V_p(\mathcal{T})$ in* (4.5)*. By introducing the semi-discrete error*

$$\mathsf{e}_N(\cdot, t) := u(\cdot, t) - u_N(\cdot, t), \qquad t \in \mathsf{J}\,, \tag{4.7}$$

we have the bound

$$\|\mathsf{e}_N\|_{\mathcal{L}^\infty(\mathsf{J};\mathcal{V}_p(\mathcal{T}))} + \|\partial_t \mathsf{e}_N\|_{\mathcal{L}^\infty(\mathsf{J};\mathcal{L}^2(\Omega))} \lesssim N^{-k/2} \|u\|_{\mathcal{C}^2(\overline{\mathsf{J}}; H^{k+1,2}_{\boldsymbol{\delta}}(\Omega))}. \tag{4.8}$$

In addition, we have the $\mathcal{L}^\infty(\mathsf{J}; \mathcal{L}^2(\Omega))$-norm error estimate

$$\|\mathsf{e}_N\|_{\mathcal{L}^\infty(\mathsf{J};\mathcal{L}^2(\Omega))} \lesssim N^{-(k+1)/2} \|u\|_{\mathcal{C}^1(\overline{\mathsf{J}}; H^{k+1,2}_{\boldsymbol{\delta}}(\Omega))}. \tag{4.9}$$

The constants $C > 0$ are independent of N.

Remark 4.4. *Note that, if* $u^0, u^1 \in \mathcal{C}_0^\infty(\Omega)$ *and* $f \in \mathcal{C}_0^\infty(\Omega \times \mathsf{J})$ *as in Proposition 2.2, then the regularity assumption* (4.6) *holds with* $k = p$. *Hence, in this case, the error bounds* (4.8) *and* (4.9) *hold true with* $k = p$, *i.e,. the SIPDG semi-discretization* (3.8) *yields quasi-optimal convergence rates in space, which are of order* $N^{-p/2}$ *in the DG energy norm and of order* $N^{-(p+1)/2}$ *in the* $\mathcal{L}^2$*-norm, as* $N \to \infty$.

Remark 4.5. *In contrast to the analysis in* [13], *our results are based on the weighted regularity shift in* (2.25). *Therefore, for the* $\mathcal{L}^2$*-norm error estimate* (4.9) *we do not need to impose any additional smoothness assumptions on the domain (or on the regularity of the interfaces for piecewise constant coefficients* c*).*

We also recall that we assume $\mathcal{D} \neq \emptyset$ *for simplicity; for the pure Neumann problem, zero energy "rigid body" related solution components must be removed by appropriate factor spaces.*

5. Proof of Theorem 4.3

In this section, we provide the proof of Theorem 4.3. We shall often use the short-hand notation $a \lesssim b$ for inequalities of the form $a \leq Cb$, where $C > 0$ is independent of the elemental mesh sizes, but may depend on κ in (3.1), on the coefficient c, on the parameter j in (3.10), the polynomial degree p, and on the particular exponent vector $\boldsymbol{\delta}$ under consideration. Also, $a \simeq b$ if $a \lesssim b$ and $b \lesssim a$.

5.1. Approximation on locally refined meshes.

We review from [25, Sects. 5.6 and 5.7] the following approximation properties on locally refined meshes.

5.1.1. *Consistency norm.* We first introduce the consistency norm which is appropriate for our analysis; cf. [25, Sect. 5.1.3].

For elements away from corners, we introduce the weighted elemental norm

$$M_K[w]^2 := h_K^{-2}\|w\|^2_{\mathcal{L}^2(K)} + \|\nabla w\|^2_{\mathcal{L}^2(K)} + h_K^2\|\mathsf{D}^2 w\|^2_{\mathcal{L}^2(K)}, \qquad K \in \mathcal{T}\backslash\mathcal{K}(\mathcal{T}). \tag{5.1}$$

For elements at corner $\mathbf{c}_i$ and $\delta_i \in [0,1)$, we set

$$N_{K,\delta_i}[w]^2 := h_K^{-2}\|w\|^2_{\mathcal{L}^2(K)} + \|\nabla w\|^2_{\mathcal{L}^2(K)} + h_K^{2-2\delta_i}|w|^2_{H^{2,2}_{\delta_i}}(K), \qquad K \in \mathcal{K}^i(\mathcal{T})\,. \tag{5.2}$$

For $\boldsymbol{\delta} \in [0,1)^{\mathsf{M}}$, we will measure consistency in the norm

$$|\!|\!| w |\!|\!|^2_{*,\boldsymbol{\delta}} := \sum_{K\in\mathcal{T}\backslash\mathcal{K}(\mathcal{T})} M_K[w]^2 + \sum_{i=1}^{\mathsf{M}} \sum_{K\in\mathcal{K}^i(\mathcal{T})} N_{K,\delta_i}[w]^2\,. \tag{5.3}$$

The DG energy norm (3.11) can be bounded by the consistency norm in (5.3); cf. [25, Lem. 5.5]. Specifically, there holds

$$|\!|\!| w |\!|\!|^2_{DG} \lesssim \sum_{K\in\mathcal{T}} \left(h_K^{-2}\|w\|^2_{\mathcal{L}^2(K)} + \|\nabla w\|^2_{\mathcal{L}^2(K)}\right), \tag{5.4}$$

for all $w \in \mathcal{V}_p(\mathcal{T})$.

5.1.2. *Approximation bounds.* We develop approximation error bounds for an abstract family of local (quasi-)interpolants $\mathcal{A} : C^0(\overline{\Omega}) \to V_p(\mathcal{T})$, which are given elementwise as $\mathcal{A}|_K = \mathcal{A}_K$ for $K \in \mathcal{T}$, with elemental interpolants

$$\mathcal{A}_K : C^0(\overline{K}) \to \mathcal{P}^p(K), \qquad K \in \mathcal{T} . \tag{5.5}$$

We suppose that $\mathcal{A}_K$ satisfies standard error bound in elements away from $\mathcal{S}$: for $1 \le k \le p$, there holds

$$M_K[w - \mathcal{A}_K w]^2 \lesssim h_K^{2k} \|\mathsf{D}^{k+1} w\|^2_{L^2(K)}, \qquad K \in \mathcal{T} \setminus \mathcal{K}(\mathcal{T}). \tag{5.6}$$

In elements K abutting at $\mathcal{S}$, we assume that

$$N_{K,\delta_i}[w - \mathcal{A}_K w]^2 \lesssim h_K^{2-2\delta_i} |w|^2_{H^{2,2}_{\delta_i}(K)}, \qquad K \in \mathcal{K}^i(\mathcal{T}). \tag{5.7}$$

Remark 5.1. *We will be working with the following two instances of elemental (quasi-)interpolants $\mathcal{A}_K : C^0(\overline{K}) \to \mathcal{P}^p(K)$ satisfying* (5.6), (5.7)*:*

(i) *(Nodal interpolation): For $K \in \mathcal{T}$, let $\mathcal{I}^p_K : \mathcal{C}^0(\overline{K}) \to \mathcal{P}^p(K)$ be the elemental nodal interpolant (at standard Lagrange nodes). Then, the bounds* (5.6) *are well-known interpolation estimates, and estimate* (5.7) *for the linear interpolant $\mathcal{I}^1_K$ is proved in* [35, Lem. 4.16]*. As in* [25]*, we introduce $\mathcal{I}_p : C^0(\overline{\Omega}) \to V_p(\mathcal{T})$ by*

$$\mathcal{I}_p w|_K := \begin{cases} \mathcal{I}^1_K(w|_K) & \text{if } K \in \mathcal{K}(\mathcal{T}) , \\ \mathcal{I}^p_K(w|_K) & \text{otherwise} . \end{cases} \tag{5.8}$$

Note that $\mathcal{I}_p : \mathcal{C}^0(\overline{\Omega}) \to V_p(\mathcal{T})$ obtained as in (5.8) *is well-defined for $w \in H^{2,2}_{\boldsymbol{\delta}}(\Omega) \hookrightarrow C(\overline{\Omega})$ due to* (2.16)*.*

(ii) *($\mathcal{L}^2$-projection): We denote by $\Pi^p_K : \mathcal{L}^2(K) \to \mathcal{P}^p(K)$ the elemental $\mathcal{L}^2$-projection on $K \in \mathcal{T}$. We then denote by $\Pi_p : \mathcal{L}^2(\Omega) \to V_p(\mathcal{T})$ the (global) $\mathcal{L}^2$-projection. Clearly, Π^p_K is well-defined on $C^0(\overline{K})$, cf.* (5.5)*, and it satisfies the error bounds in* (5.6)*. The approximation estimate* (5.7) *follows from a minor modification of* [34, Lem. 8.4] *where this result was shown for quadrilateral corner elements and tensor-product polynomial spaces. For the sake of completeness, we present a proof.*

Lemma 5.2. *For $1 \le i \le \mathsf{M}$, let $K \in \mathcal{K}^i(\mathcal{T})$ and $w \in H^{2,2}_{\delta_i}(K)$. Then, for any polynomial degree $p \ge 1$, there holds*

$$N_{K,\delta_i}[w - \Pi^p_K w]^2 \le C h_K^{2-2\delta_i} |w|^2_{H^{2,2}_{\delta_i}(K)}, \tag{5.9}$$

with $C > 0$ independent of the elemental mesh sizes, but depending on p.

Proof. Let $\widehat{K}$ be a reference triangle of unit size and denote by $\widehat{\Pi}^p$ the $\mathcal{L}^2$-projection onto the polynomial space $\mathcal{P}^p(\widehat{K})$. We first claim that

$$\|\widehat{\mathsf{D}}^k(\widehat{\Pi}^p \widehat{w})\|^2_{\mathcal{L}^2(\widehat{K})} \lesssim \max\{p,1\}^{4k} \|\widehat{\mathsf{D}}^k \widehat{w}\|^2_{\mathcal{L}^2(\widehat{K})}, \quad p \ge 0 , \ k \ge 0 , \tag{5.10}$$

see also [34, Lem. 4.1]. Here we note that (5.10) holds trivially for $k \ge p+1$ (since then $\mathsf{D}^k(\widehat{\Pi}^p \widehat{w}) = 0$). Note further that the case $k = 0$ follows from the $\mathcal{L}^2$-stability of $\widehat{\Pi}^p$ with constant one. This already implies the result for $p = 0$, and it remains to consider the case $1 \le k \le p$. Then, we have

$\widehat{\mathsf{D}}^k(\widehat{\Pi}^p\widehat{w}) = \widehat{\mathsf{D}}^k\widehat{\Pi}^p(\widehat{w}-\widehat{\Pi}^{k-1}\widehat{w})$. With the inverse estimate in [35, Thm. 4.76] and standard approximation properties, we conclude that

$$\|\widehat{\mathsf{D}}^k(\widehat{\Pi}^p\widehat{w})\|^2_{\mathcal{L}^2(\widehat{K})} \lesssim p^{4k}\|\widehat{w}-\widehat{\Pi}^{k-1}\widehat{w}\|^2_{\mathcal{L}^2(\widehat{K})} \lesssim \|\widehat{\mathsf{D}}^k\widehat{w}\|^2_{\mathcal{L}^2(\widehat{K})}\,,$$

which is (5.10) for $1 \le k \le p$.

With this auxiliary result in place, we now establish (5.9). Again, we first consider the reference triangle $\widehat{K}$. Let $p \ge 1$. Applying (5.10) for $k = 0, 1, 2$, we see that

$$\begin{aligned}\|\widehat{w}-\widehat{\Pi}^p\widehat{w}\|^2_{H^2(\widehat{K})} &\lesssim \|\widehat{w}-\widehat{\Pi}^1\widehat{w}\|^2_{H^2(\widehat{K})} + \|\widehat{\Pi}^p(\widehat{w}-\widehat{\Pi}^1\widehat{w})\|^2_{H^2(\widehat{K})}\\ &\lesssim p^8\|\widehat{w}-\widehat{\Pi}^1\widehat{w}\|^2_{H^2(\widehat{K})}.\end{aligned}$$

As we are interested in convergence rate estimates for $h \to 0$, it now suffices to prove (5.9) for $\widehat{\Pi}^1$, i.e., for $p = 1$. To do so, we next claim that there is a constant $\widehat{C} > 0$ independent of $\widehat{w}$ such that

$$\|\widehat{w}\|_{H^{2,2}_{\delta_i}(\widehat{K})} \le \widehat{C}\big(|\widehat{w}|_{H^{2,2}_{\delta_i}(\widehat{K})} + \|\widehat{\Pi}^1\widehat{w}\|_{\mathcal{L}^2(\widehat{K})}\big)\,. \tag{5.11}$$

The bound (5.11) follows with standard arguments from the Peetre-Tartar lemma (see [10, Lem. A.38]) and the fact that the embedding $H^{2,2}_{\delta_i}(\widehat{K}) \hookrightarrow H^1(\widehat{K})$ is compact (see [15, Lem. 3.4]). Applying (5.11) to $\widehat{w}-\widehat{\Pi}^1\widehat{w}$ and noting that $|\widehat{\Pi}^1\widehat{w}|_{H^{2,2}_{\delta_i}(\widehat{K})} = 0$, $\widehat{\Pi}^1(\widehat{w}-\widehat{\Pi}^1\widehat{w}) = 0$ result in

$$\|\widehat{w}-\widehat{\Pi}^1\widehat{w}\|_{H^{2,2}_{\delta_i}(\widehat{K})} \le \widehat{C}|\widehat{w}|_{H^{2,2}_{\delta_i}(\widehat{K})}, \tag{5.12}$$

which is (5.9) on the reference element $\widehat{K}$. For a general element $K \in \mathcal{K}^i(\mathcal{T})$, the desired bound in (5.9) follows from (5.12) and a scaling argument. This finishes the proof. □

We are now in position to state the convergence rate estimates on locally refined triangulations in Ω.

Proposition 5.3. *Let $p \ge 1$ and $\boldsymbol{\delta} \in [0,1)^{\mathsf{M}}$. Consider a family of locally refined meshes $\mathcal{T}$ as in Definition 4.1. For $1 \le k \le p$, let $w \in H^{k+1,2}_{\boldsymbol{\delta}}(\Omega)$ and let $\mathcal{A}v$ be a local (quasi-)interpolant as in* (5.5)*, which satisfies* (5.6)*,* (5.7)*. Then we have*

$$|||w-\mathcal{A}w|||_{*,\boldsymbol{\delta}} \le CN^{-k/2}|w|_{H^{k+1,2}_{\boldsymbol{\delta}}(\Omega)}\,, \tag{5.13}$$

with a constant $C > 0$ independent of N.

Proof. In [25, Props. 5.17 and 5.18], this was proved for the nodal interpolant $\mathcal{I}_p$ in (5.8) for graded and bisection refinement meshes, respectively. Careful inspection of the proofs there reveals that the estimate (5.13) remains valid for generic approximants $\mathcal{A}$ as in (5.5) provided that the error bounds (5.6) and (5.7) are fulfilled. □

5.2. **Boundedness.** Next, we review the continuity of the DG form $a_{DG}(\cdot,\cdot)$. The following result was established in [25, Prop. 5.7], by employing Lemma 3.1 to handle corner weights.

Proposition 5.4. *Let $\boldsymbol{\delta}, \boldsymbol{\delta}' \in [0,1)^{\mathsf{M}}$. Then:*

(i) *For $w = w_0 + w_N$ with $w_0 \in H^{2,2}_{\boldsymbol{\delta}}(\Omega)$ and $w_N \in V_p(\mathcal{T})$, we have*

$$|a_{DG}(w, v_N)| \le C_{A,1} |\!|\!| w |\!|\!|_{*,\boldsymbol{\delta}} |\!|\!| v_N |\!|\!|_{DG} \,, \qquad v_N \in V_p(\mathcal{T}) \,. \tag{5.14}$$

(ii) *For $w = w_0 + w_N$ and $v = v_0 + v_N$ with $w_0 \in H^{2,2}_{\boldsymbol{\delta}}(\Omega)$, $v_0 \in H^{2,2}_{\boldsymbol{\delta}'}(\Omega)$ and $w_N, v_N \in V_p(\mathcal{T})$, we have*

$$|a_{DG}(w, v)| \le C_{A,2} |\!|\!| w |\!|\!|_{*,\boldsymbol{\delta}} |\!|\!| v |\!|\!|_{*,\boldsymbol{\delta}'} \,. \tag{5.15}$$

The constants $C_{A,1} > 0$ and $C_{A,2} > 0$ are independent of the elemental mesh sizes.

We further recall the following integration-by-parts formula; cf. [25, Lem. 5.12].

Lemma 5.5. *Let $\boldsymbol{\delta}, \boldsymbol{\delta}' \in [0,1)^{\mathsf{M}}$. For $w \in H^{2,2}_{\boldsymbol{\delta}}(\Omega)$, we have $\mathsf{c}\nabla w \in H^{1,1}_{\boldsymbol{\delta}}(\Omega)^2$, $\nabla \cdot (\mathsf{c}\nabla w) \in H^{0,0}_{\boldsymbol{\delta}}(\Omega)$ and*

$$\sum_{K\in\mathcal{T}} \int_K \mathsf{c}\nabla w \cdot \nabla v \, d\mathbf{x} = -\sum_{K\in\mathcal{T}} \int_K \nabla\cdot(\mathsf{c}\nabla w) v \, d\mathbf{x} + \sum_{e\in\mathcal{E}_{\mathcal{T}}} \int_e [\![v]\!] \cdot \langle\!\langle \mathsf{c}\nabla w \rangle\!\rangle \, dS \,, \tag{5.16}$$

for any $v = v_0 + v_N$ with $v_0 \in H^{2,2}_{\boldsymbol{\delta}'}(\Omega)$ and $v_N \in V_p(\mathcal{T})$. For corner elements K, the volume integrals are well-defined over $\mathcal{L}^1(K) \times \mathcal{L}^\infty(K)$ and the integrals over edges $e \in \mathcal{E}_{\mathcal{T}}$ running into corners are well-defined over $\mathcal{L}^1(e) \times \mathcal{L}^\infty(e)$; see the embedding (2.16) *and Lemma 3.1.*

5.3. **Galerkin projection.** For $\boldsymbol{\delta} \in [0,1)^{\mathsf{M}}$ and $w \in H^{2,2}_{\boldsymbol{\delta}}(\Omega)$, the Galerkin projection $\mathcal{G}_p w \in V_p(\mathcal{T})$ is defined by

$$\mathcal{G}_p w \in V_p(\mathcal{T}) : \quad a_{DG}(\mathcal{G}_p w, v_N) = a_{DG}(w, v_N) \qquad \forall\, v_N \in V_p(\mathcal{T}) \,. \tag{5.17}$$

Note that $\mathcal{G}_p w$ is well-defined and, in view of the coercivity (3.12) and the continuity bound (5.14), that there holds

$$|\!|\!| \mathcal{G}_p w |\!|\!|_{DG} \le C_{coer}^{-1} C_{A,1} |\!|\!| w |\!|\!|_{*,\boldsymbol{\delta}}. \tag{5.18}$$

In addition, we clearly have

$$a_{DG}(w - \mathcal{G}_p w, v_N) = 0, \qquad v_N \in V_p(\mathcal{T}), \tag{5.19}$$

Moreover, it can be easily seen that $\mathcal{G}_p$ reproduces DG functions, i.e.,

$$\mathcal{G}_p w_N = w_N, \qquad w_N \in V_p(\mathcal{T}) \,. \tag{5.20}$$

5.3.1. *Energy norm approximation.* The following DG energy norm approximation bound is proved as in [25, Lem. 5.15].

Lemma 5.6. *For $p \ge 1$ and $\boldsymbol{\delta} \in [0,1)^{\mathsf{M}}$, let $w \in H^{2,2}_{\boldsymbol{\delta}}(\Omega)$ and let $\mathcal{G}_p w \in V_p(\mathcal{T})$ be the Galerkin projection in* (5.17)*. Then we have the energy norm bound*

$$|\!|\!| w - \mathcal{G}_p w |\!|\!|_{DG} \lesssim \inf_{v_N \in V_p(\mathcal{T})} |\!|\!| w - v_N |\!|\!|_{*,\boldsymbol{\delta}} \,. \tag{5.21}$$

5.3.2. *$\mathcal{L}^2$-norm approximation.* To prove an $\mathcal{L}^2$-norm approximation result for $\mathcal{G}_p w$, we consider the dual problem

$$-\nabla\cdot(\mathsf{c}\nabla z) = w - \mathcal{G}_p w \qquad \text{in } \Omega \,, \tag{5.22}$$

$$z = 0 \qquad \text{on } \Gamma_D \,, \tag{5.23}$$

$$\boldsymbol{\nu}\cdot(\mathsf{c}\nabla z) = 0 \qquad \text{on } \Gamma_N \,. \tag{5.24}$$

Let $\boldsymbol{\delta} \in [0,1)^{\mathsf{M}}$ be as in (2.21). Then, the regularity shift in (2.25) shows that $z \in H^{2,2}_{\boldsymbol{\delta}}(\Omega)$ and

$$\|z\|_{H^{2,2}_{\boldsymbol{\delta}}(\Omega)} \leq C_{stab,2}\|w - \mathcal{G}_p w\|_{H^{0,0}_{\boldsymbol{\delta}}(\Omega)} \leq C\|w - \mathcal{G}_p w\|_{\mathcal{L}^2(\Omega)}. \tag{5.25}$$

As in [25, Lem. 5.16], we obtain the following result.

Lemma 5.7. *Let $p \geq 1$ and $\boldsymbol{\delta} \in [0,1)^{\mathsf{M}}$ as in (2.21). Let $w \in H^{2,2}_{\boldsymbol{\delta}}(\Omega)$ and let $\mathcal{G}_p w \in V_p(\mathcal{T})$ be the Galerkin projection in (5.17). Let $z \in H^{2,2}_{\boldsymbol{\delta}}(\Omega)$ be the dual solution of (5.22)–(5.24). Assume the approximation property*

$$\inf_{z_N \in V_p(\mathcal{T})} |\!|\!| z - z_N |\!|\!|_{*,\boldsymbol{\delta}} \leq C_{approx} d(p, \mathcal{T}, \boldsymbol{\delta}) \|z\|_{H^{2,2}_{\boldsymbol{\delta}}(\Omega)}. \tag{5.26}$$

Then we have the $\mathcal{L}^2$-norm bound

$$\|w - \mathcal{G}_p w\|_{\mathcal{L}^2(\Omega)} \leq C d(p, \mathcal{T}, \boldsymbol{\delta}) \inf_{v_N \in V_p(\mathcal{T})} |\!|\!| w - v_N |\!|\!|_{*,\boldsymbol{\delta}}\ , \tag{5.27}$$

with a constant $C > 0$ independent of the elemental mesh sizes.

Proof. We test (5.22) with $w - \mathcal{G}_p w$, integrate by parts with the aid of (5.16), and use the Neumann boundary conditions (5.24) and the fact that $[\![z]\!]|_e = \mathbf{0}$ for all $e \in \mathcal{E}^{\circ}_{\mathcal{T}} \cup \mathcal{E}^{\mathcal{D}}_{\mathcal{T}}$. This yields

$$\begin{aligned} \|w - \mathcal{G}_p w\|^2_{\mathcal{L}^2(\Omega)} &= \sum_{K \in \mathcal{T}} \int_K \mathsf{c}\nabla z \cdot \nabla(w - \mathcal{G}_p w)\, d\mathbf{x} - \sum_{e \in \mathcal{E}_{\mathcal{T}}} \int_e [\![w - \mathcal{G}_p w]\!] \cdot \langle\!\langle \mathsf{c}\nabla z \rangle\!\rangle\, dS \\ &= a_{DG}(z, w - \mathcal{G}_p w), \end{aligned}$$

where all the integrals over edges are well-defined as in (5.16) and (5.15). We now proceed analogously to [25, Lem. 5.16]. That is, we invoke the symmetry of $a_{DG}(\cdot,\cdot)$, the orthogonality (5.19), the continuity bound (5.15), the approximation assumption (5.26) and the stability bound (5.25). The estimate (5.27) readily follows. □

Consequently, the following approximation properties hold for the Galerkin projection in (5.17):

Proposition 5.8. *Let $p \geq 1$ and $\boldsymbol{\delta} \in [0,1)^{\mathsf{M}}$ as in (2.21). Consider a family of meshes $\mathcal{T}$, which are locally refined towrds $\mathcal{S}$ with respect to $\boldsymbol{\delta}$ and p as in Definition 4.1. For $1 \leq k \leq p$, let $w \in H^{k+1,2}_{\boldsymbol{\delta}}(\Omega)$ and let $\mathcal{G}_p w$ be the Galerkin projection of w defined in (5.17). Then there holds*

$$|\!|\!| w - \mathcal{G}_p w |\!|\!|_{DG} + N^{1/2}\|w - \mathcal{G}_p w\|_{\mathcal{L}^2(\Omega)} \lesssim N^{-k/2}|w|_{H^{k+1,2}_{\boldsymbol{\delta}}(\Omega)}\ . \tag{5.28}$$

Proof. This follows from the bounds in Lemma 5.6 (DG energy norm error) and Lemma 5.7 ($\mathcal{L}^2$-norm error), in conjunction with the approximation properties in Proposition 5.3 for the nodal interpolant $\mathcal{I}_p$ in (5.8) and by noting that $d(p, \mathcal{T}, \boldsymbol{\delta}) \leq CN^{-1/2}$ in (5.26), due to (5.13) for $\mathcal{I}_p$. □

5.4. **Error estimates.** We now derive semi-discrete error estimates in space.

5.4.1. *Error equations.* We first discuss the error equations.

Lemma 5.9. *For $\boldsymbol{\delta} \in [0,1)^{\mathsf{M}}$, let the solution u of (2.4)–(2.8) satisfy the regularity assumption*

$$u \in \mathcal{C}^2(\overline{\mathsf{J}}; H^{2,2}_{\boldsymbol{\delta}}(\Omega)) \tag{5.29}$$

Let $u_N \in \mathcal{C}^2(\overline{\mathsf{J}}; V_p(\mathcal{T}))$ be the semi-discrete solution obtained by (3.8) with $\mathsf{j} > \mathsf{j}_*$ and consider the error $\mathsf{e}_N(\cdot,t) = u(\cdot,t) - u_N(\cdot,t)$. Then we have

$$(\partial_t^2 \mathsf{e}_N(t), v) + a_{DG}(\mathsf{e}_N(t), v) = 0 \,, \tag{5.30}$$

for all $t \in \mathsf{J}$ and $v \in V_p(\mathcal{T})$.

Proof. For fixed $t \in \mathsf{J}$, we test the equation (2.4) with $v \in V_p(\mathcal{T})$ and use integration-by-parts as in (5.16). This results in

$$\sum_{K\in\mathcal{T}} \int_K f v \, d\mathbf{x} = \sum_{K\in\mathcal{T}} \int_K \mathsf{c}\nabla u \cdot \nabla v \, d\mathbf{x} - \sum_{e\in\mathcal{E}_\mathcal{T}} \int_e [\![v]\!] \cdot \langle\!\langle \mathsf{c}\nabla u \rangle\!\rangle \, dS \,. \tag{5.31}$$

Since $[\![u]\!]|_e = \mathbf{0}$ in $\mathcal{L}^2(e)^2$ for $e \in \mathcal{E}_\mathcal{T}^\circ \cup \mathcal{E}_\mathcal{T}^\mathcal{D}$ and $[\![\mathsf{c}\nabla u]\!]|_e = 0$ in $\mathcal{L}^1(e)^2$ for $e \in \mathcal{E}_\mathcal{T}^\circ \cup \mathcal{E}_\mathcal{T}^\mathcal{N}$, we readily find that

$$\sum_{K\in\mathcal{T}} \int_K f v \, d\mathbf{x} = a_{DG}(u,v),$$

which in turn implies the error equation (5.30). □

5.4.2. *Galerkin projection in space.* For $w \in \mathcal{C}^0(\overline{\mathsf{J}}; H^{2,2}_{\boldsymbol{\delta}}(\Omega))$, we apply the Galerkin projection in space by setting

$$a_{DG}(\mathcal{G}_p w(t), v) = a_{DG}(w(t), v), \tag{5.32}$$

for all $t \in \mathsf{J}$ and $v \in V_p(\mathcal{T})$. We have $\mathcal{G}_p w \in \mathcal{C}^0(\overline{\mathsf{J}}; V_p(\mathcal{T}))$ and

$$(\mathcal{G}_p w)(0) = \mathcal{G}_p(w(0)) \,. \tag{5.33}$$

In addition, if also $\partial_t w \in \mathcal{C}^0(\overline{\mathsf{J}}; H^{2,2}_{\boldsymbol{\delta}}(\Omega))$, then $\partial_t \mathcal{G}_p w \in \mathcal{C}^0(\overline{\mathsf{J}}; V_p(\mathcal{T}))$ and

$$\partial_t \mathcal{G}_p w(t) = \mathcal{G}_p\big(\partial_t w(t)\big), \qquad t \in \overline{\mathsf{J}}. \tag{5.34}$$

Let now $u \in \mathcal{C}^2(\overline{\mathsf{J}}; H^{2,2}_{\boldsymbol{\delta}}(\Omega))$ be the solution of (2.4)–(2.8), $\mathcal{G}_p u$ its Galerkin projection in (5.32), and $u_N \in \mathcal{C}^2(\overline{\mathsf{J}}; V_p(\mathcal{T}))$ the semi-discretization obtained by (3.8) with $\mathsf{j} > \mathsf{j}_*$. We split the error $\mathsf{e}_N = u - u_N$ into

$$\mathsf{e}_N(t) = \big(u(t) - \mathcal{G}_p u(t)\big) + \big(\mathcal{G}_p u(t) - u_N(t)\big) =: \eta(t) + \xi(t), \qquad t \in \overline{\mathsf{J}}. \tag{5.35}$$

Then the following result holds.

Lemma 5.10. *Let $u \in \mathcal{C}^2(\overline{\mathsf{J}}; H^{2,2}_{\boldsymbol{\delta}}(\Omega))$. With (5.35), there holds*

$$(\partial_t^2 \xi, v) + a_{DG}(\xi, v) = -(\partial_t^2 \eta, v) \,, \tag{5.36}$$

for all $t \in \mathsf{J}$ and $v \in V_p(\mathcal{T})$.

Proof. The splitting (5.35), the error equation (5.30) and the definition (5.32) imply

$$(\partial_t^2 \xi, v) + a_{DG}(\xi, v) = (\partial_t^2 \mathsf{e}_N, v) + a_{DG}(\mathsf{e}_N, v) - (\partial_t^2 \eta, v) - a_{DG}(\eta, v) = -(\partial_t^2 \eta, v),$$

which finishes the proof. □

5.4.3. *Error bounds.* We next prove the following error bounds.

Proposition 5.11. *Let $\boldsymbol{\delta} \in [0,1)^{\mathsf{M}}$. Let the solution u of (2.4)–(2.8) satisfy the regularity assumption*

$$u \in \mathcal{C}^2(\overline{\mathsf{J}}; H^{2,2}_{\boldsymbol{\delta}}(\Omega)) \tag{5.37}$$

Let u_N be the semi-discretization obtained by (3.8) with $\mathsf{j} > \mathsf{j}_*$ and with the discrete initial data $u_N^0, u_N^1 \in V_p(\mathcal{T})$ in (4.5):

$$u_N^0 = \Pi_p u^0, \qquad u_N^1 = \Pi_p u^1. \tag{5.38}$$

Let the error $\mathsf{e}_N = \eta + \xi$ be split as in (5.35). Then we have

$$\begin{aligned} \|\mathsf{e}_N\|_{\mathcal{L}^\infty(\mathsf{J};\mathcal{V}_p(\mathcal{T}))} + \|\partial_t \mathsf{e}_N\|_{\mathcal{L}^\infty(\mathsf{J};\mathcal{L}^2(\Omega))} \le C\big(&|\!|\!| u^0 - \Pi_p u^0 |\!|\!|_{*,\boldsymbol{\delta}} \\ &+ \|u^1 - \mathcal{G}_p u^1\|_{\mathcal{L}^2(\Omega)} + \|\eta\|_{\mathcal{L}^\infty(\mathsf{J};\mathcal{V}_p(\mathcal{T}))} \\ &+ \|\partial_t \eta\|_{\mathcal{L}^\infty(\mathsf{J};\mathcal{L}^2(\Omega))} + \|\partial_t^2 \eta\|_{\mathcal{L}^1(\mathsf{J};\mathcal{L}^2(\Omega))}\big)\,. \end{aligned} \tag{5.39}$$

In addition, the $\mathcal{L}^\infty(\mathsf{J};\mathcal{L}^2(\Omega))$-norm error is bounded by

$$\begin{aligned} \|\mathsf{e}_N\|_{\mathcal{L}^\infty(\mathsf{J};\mathcal{L}^2(\Omega))} \le C\big(&\|u^0 - \mathcal{G}_p u^0\|_{\mathcal{L}^2(\Omega)} \\ &+ \|\eta\|_{\mathcal{L}^\infty(\mathsf{J};\mathcal{L}^2(\Omega))} + \|\partial_t \eta\|_{\mathcal{L}^\infty(\mathsf{J};\mathcal{L}^2(\Omega))}\big). \end{aligned} \tag{5.40}$$

The constants $C > 0$ are independent of the elemental mesh sizes.

Proof. We show (5.39): With (5.35) and the triangle inequality, we have

$$\|\mathsf{e}_N\|_{\mathcal{L}^\infty(\mathsf{J};\mathcal{V}_p(\mathcal{T}))} + \|\partial_t \mathsf{e}_N\|_{\mathcal{L}^\infty(\mathsf{J};\mathcal{L}^2(\Omega))} \le E_1 + E_2, \tag{5.41}$$

where

$$E_1 = \|\eta\|_{\mathcal{L}^\infty(\mathsf{J};\mathcal{V}_p(\mathcal{T}))} + \|\partial_t \eta\|_{\mathcal{L}^\infty(\mathsf{J};\mathcal{L}^2(\Omega))}\,, \quad E_2 = \|\xi\|_{\mathcal{L}^\infty(\mathsf{J};\mathcal{V}_p(\mathcal{T}))} + \|\partial_t \xi\|_{\mathcal{L}^\infty(\mathsf{J};\mathcal{L}^2(\Omega))}\,.$$

It remains to bound E_2. To this end, we choose $v(t) = \partial_t \xi(t) \in V_p(\mathcal{T})$ in (5.36) and use the symmetry of $a_{DG}(\cdot,\cdot)$. This yields

$$\frac{1}{2}\frac{d}{dt}\Big(\|\partial_t \xi\|^2_{\mathcal{L}^2(\Omega)} + a_{DG}(\xi,\xi)\Big) = -(\partial_t^2 \eta, \partial_t \xi), \qquad t \in \mathsf{J}.$$

Fix $s \in \mathsf{J}$. By integrating the equation above with respect to t over $(0,s)$, we see that

$$\begin{aligned} \frac{1}{2}\|\partial_t \xi(s)\|^2_{\mathcal{L}^2(\Omega)} + \frac{1}{2} a_{DG}(\xi(s),\xi(s))^2 \le \frac{1}{2}\|\partial_t \xi(0)\|^2_{\mathcal{L}^2(\Omega)} + \frac{1}{2} a_{DG}(\xi(0),\xi(0)) \\ + \int_0^s |(\partial_t^2 \eta, \partial_t \xi)|\, dt. \end{aligned}$$

With the inequalities of Hölder and Young, we have

$$\begin{aligned} \int_0^s |(\partial_t^2 \eta, \partial_t \xi)|\, dt &\le \|\partial_t \xi\|_{\mathcal{L}^\infty(\mathsf{J};\mathcal{L}^2(\Omega))} \|\partial_t^2 \eta\|_{\mathcal{L}^1(\mathsf{J};\mathcal{L}^2(\Omega))} \\ &\le \frac{\varepsilon}{2}\|\partial_t \xi\|^2_{\mathcal{L}^\infty(\mathsf{J};\mathcal{L}^2(\Omega))} + \frac{1}{2\varepsilon}\|\partial_t^2 \eta\|^2_{\mathcal{L}^1(\mathsf{J};\mathcal{L}^2(\Omega))}\,, \end{aligned}$$

for any $\varepsilon > 0$. Hence, combined with the coercivity (3.12) and continuity (3.13) of the form $a_{DG}(\cdot,\cdot)$, we find that

$$\begin{aligned} \|\partial_t \xi(s)\|^2_{\mathcal{L}^2(\Omega)} + C_{coer}|\!|\!|\xi(s)|\!|\!|^2_{DG} \le \|\partial_t \xi(0)\|^2_{\mathcal{L}^2(\Omega)} + C_{cont}|\!|\!|\xi(0)|\!|\!|^2_{DG} \\ + \varepsilon\|\partial_t \xi\|^2_{\mathcal{L}^\infty(\mathsf{J};\mathcal{L}^2(\Omega))} + \varepsilon^{-1}\|\partial_t^2 \eta\|^2_{\mathcal{L}^1(\mathsf{J};\mathcal{L}^2(\Omega))}\,. \end{aligned}$$

Since this holds for any $s \in \mathsf{J}$, it also holds for the respective suprema over J. Then, choosing ε sufficiently small allows us to absorb the term $\varepsilon\|\partial_t\xi\|^2_{\mathcal{L}^\infty(\mathsf{J};\mathcal{L}^2(\Omega))}$ in the left-hand side, which results in

$$\begin{aligned} E_2^2 &\simeq \|\partial_t\xi\|^2_{\mathcal{L}^\infty(\mathsf{J};\mathcal{L}^2(\Omega))} + \|\xi\|^2_{\mathcal{L}^\infty(\mathsf{J};\mathcal{V}_p(\mathcal{T}))} \\ &\lesssim \|\partial_t\xi(0)\|^2_{\mathcal{L}^2(\Omega)} + |\!|\!|\xi(0)|\!|\!|^2_{DG} + \|\partial_t^2\eta\|^2_{\mathcal{L}^1(\mathsf{J};\mathcal{L}^2(\Omega))}. \end{aligned} \tag{5.42}$$

Consider now discrete initial data $u_N^0, u_N^1 \in V_p(\mathcal{T})$ in (5.38). Then, with (5.33) and (5.20), we notice that $\xi(0) = \mathcal{G}_p u^0 - \Pi_p u^0 = \mathcal{G}_p(u^0 - \Pi_p u^0)$. Hence, from the stability property (5.18), we see that

$$|\!|\!|\xi(0)|\!|\!|_{DG} = |\!|\!|\mathcal{G}_p(u^0 - \Pi_p u^0)|\!|\!|_{DG} \lesssim |\!|\!|u^0 - \Pi_p u^0|\!|\!|_{*,\boldsymbol{\delta}} \,.$$

Moreover, with (5.34), we see that $\partial_t\xi(0) = \mathcal{G}_p u^1 - \Pi_p u^1 = \Pi_p(\mathcal{G}_p u^1 - u^1)$. The stability of the $\mathcal{L}^2$-projection yields $\|\partial_t\xi(0)\|_{\mathcal{L}^2(\Omega)} \le \|u^1 - \mathcal{G}_p u^1\|_{\mathcal{L}^2(\Omega)}$. Hence, we conclude from (5.42) that

$$E_2^2 \lesssim |\!|\!|u^0 - \Pi_p u^0|\!|\!|^2_{*,\boldsymbol{\delta}} + \|u^1 - \mathcal{G}_p u^1\|^2_{\mathcal{L}^2(\Omega)} + \|\partial_t^2\eta\|^2_{\mathcal{L}^1(\mathsf{J};\mathcal{L}^2(\Omega))}. \tag{5.43}$$

The definition of E_1 and the bound (5.43) imply the error estimate (5.39). Next, we establish (5.40). From the splitting (5.35), we obtain

$$\|\mathsf{e}_N\|_{\mathcal{L}^\infty(\mathsf{J};\mathcal{L}^2(\Omega))} \le \|\eta\|_{\mathcal{L}^\infty(\mathsf{J};\mathcal{L}^2(\Omega))} + \|\xi\|_{\mathcal{L}^\infty(\mathsf{J};\mathcal{L}^2(\Omega))} \,.$$

To bound $\|\xi\|_{\mathcal{L}^\infty(\mathsf{J};\mathcal{L}^2(\Omega))}$, we proceed as in the proof of [13, Thm. 4.2]. That is, we first rewrite (5.36) as

$$\frac{d}{dt}(\partial_t\xi, v) - (\partial_t\xi, \partial_t v) + a_{DG}(\xi, v) = -\frac{d}{dt}(\partial_t\eta, v) + (\partial_t\eta, \partial_t v),$$

and use that $\mathsf{e}_N = \eta + \xi$, which results in the identity

$$-(\partial_t\xi, \partial_t v) + a_{DG}(\xi, v) = -\frac{d}{dt}(\partial_t\mathsf{e}_N, v) + (\partial_t\eta, \partial_t v), \tag{5.44}$$

for all $t \in \mathsf{J}$ and $v \in V_p(\mathcal{T})$. Then, for $\tau \in \mathsf{J}$, we define the function

$$v(\cdot, t) = \int_t^\tau \xi(\cdot, s)\, ds, \qquad t \in \mathsf{J}.$$

Note that $v(\cdot, t) \in V_p(\mathcal{T})$ and

$$v(\cdot, \tau) = 0, \qquad \partial_t v(\cdot, t) = -\xi(t). \tag{5.45}$$

We choose $v(\cdot, t)$ in (5.44) and employ (5.45) as well as the symmetry of $a_{DG}(\cdot,\cdot)$ to obtain

$$\frac{1}{2}\frac{d}{dt}\|\xi\|^2_{\mathcal{L}^2(\Omega)} - \frac{1}{2}\frac{d}{dt}a_{DG}(v, v) = -\frac{d}{dt}(\partial_t\mathsf{e}_N, v) - (\partial_t\eta, \xi).$$

By integrating this identity over $(0, \tau)$, using that $v(\cdot, \tau) = 0$ and the fact that $a_{DG}(v(0), v(0)) \ge 0$ due to (3.12), and by applying the Cauchy-Schwarz inequality, we conclude that

$$\|\xi(\tau)\|^2_{\mathcal{L}^2(\Omega)} \le \|\xi(0)\|^2_{\mathcal{L}^2(\Omega)} + 2|(\partial_t\mathsf{e}_N(0), v(0))| + 2\int_{\mathsf{J}} \|\partial_t\eta\|_{\mathcal{L}^2(\Omega)}\|\xi\|_{\mathcal{L}^2(\Omega)}\, dt.$$

Since the above bound holds for any $\tau \in \mathsf{J}$, it also holds for $\|\xi\|_{\mathcal{L}^\infty(\mathsf{J};\mathcal{L}^2(\Omega))}$. From (5.38) and since Π_p reproduces functions in $V_p(\mathcal{T})$, we have as before that

$\xi(0) = \mathcal{G}_p u^0 - \Pi_p u^0 = \Pi_p(\mathcal{G}_p u^0 - u^0)$. The stability of the $\mathcal{L}^2$-projection thus implies

$$\|\xi(0)\|_{\mathcal{L}^2(\Omega)} \leq \|u^0 - \mathcal{G}_p u^0\|_{\mathcal{L}^2(\Omega)}.$$

In addition, $u_N^1 = \Pi_p u^1$ so that $(\partial_t \mathsf{e}_N(0), v(0)) = (u^1 - \Pi_p u^1, v(0)) = 0$. The last term above is bounded with the help of the weighted Cauchy-Schwarz inequality as follows

$$2\int_{\mathsf{J}} \|\partial_t \eta\|_{\mathcal{L}^2(\Omega)} \|\xi\|_{\mathcal{L}^2(\Omega)}\, dt \leq \frac{1}{2}\|\xi\|^2_{\mathcal{L}^\infty(\mathsf{J};\mathcal{L}^2(\Omega))} + C\|\partial_t \eta\|^2_{\mathcal{L}^\infty(\mathsf{J};\mathcal{L}^2(\Omega)}.$$

Combining these arguments and bringing the first term above to the left-hand side implies (5.40). □

5.5. **Proof of Theorem 4.3.** For $\boldsymbol{\delta} \in [0,1)^{\mathsf{M}}$ and $k \in \mathbb{N}$, we write $\mathcal{C}^k(\overline{\mathsf{J}}; \|\!|\cdot|\!\|_{*,\boldsymbol{\delta}})$for all functions $w : \Omega \to \mathbb{R}$ which are k-times continuously differentiable in $t \in \overline{\mathsf{J}}$ with finite norm $\|\!|\cdot|\!\|_{*,\boldsymbol{\delta}}$ in space, i.e.,

$$\|w\|_{\mathcal{C}^k(\overline{\mathsf{J}};\|\!|\cdot|\!\|_{*,\boldsymbol{\delta}})} := \sum_{m=0}^{k} \sup_{t\in\overline{\mathsf{J}}} \|\!|\partial_t^m w|\!\|_{*,\boldsymbol{\delta}} < \infty\,. \tag{5.46}$$

With this definition at hand, we now complete the proof of Theorem 4.3. To do so, let $\boldsymbol{\delta} \in [0,1)^{\mathsf{M}}$ be as in (2.20). Then, from the error bound (5.39) and the regularity assumptions (5.37), (4.6) and the definition of the consistency norm (5.3), it follows that

$$\|\mathsf{e}_N\|_{\mathcal{L}^\infty(\mathsf{J};\mathcal{V}_p(\mathcal{T}))} + \|\partial_t \mathsf{e}_N\|_{\mathcal{L}^\infty(\mathsf{J};\mathcal{L}^2(\Omega))} \leq C\big(\|\!|u^0 - \Pi_p u^0|\!\|_{*,\boldsymbol{\delta}} + \|u - \mathcal{G}_p u\|_{\mathcal{C}^2(\overline{\mathsf{J}};\|\!|\cdot|\!\|_{*,\boldsymbol{\delta}})}\big)\,.$$

The approximation results for the Galerkin projection in Proposition 5.8 (along with (5.34)) imply

$$\|u - \mathcal{G}_p u\|_{\mathcal{C}^2(\overline{\mathsf{J}};\|\!|\cdot|\!\|_{*,\boldsymbol{\delta}})} \lesssim N^{-k/2}\|u\|_{\mathcal{C}^2(\overline{\mathsf{J}};H^{k+1,2}_{\boldsymbol{\delta}}(\Omega))}.$$

Proposition 5.3 for the $\mathcal{L}^2$-projection Π_p shows that

$$\|\!|u^0 - \Pi_p u^0|\!\|_{*,\boldsymbol{\delta}} \lesssim N^{-k/2}|u^0|_{H^{k+1,2}_{\boldsymbol{\delta}}(\Omega)}\,.$$

These arguments yield the energy norm bound (4.8).

Similarly, with (5.40), (5.34) and Proposition 5.8, we obtain

$$\|\mathsf{e}_N\|_{\mathcal{L}^\infty(\mathsf{J};\mathcal{L}^2(\Omega))} \leq C\|\eta\|_{\mathcal{C}^1(\overline{\mathsf{J}};\mathcal{L}^2(\Omega))} \leq CN^{-(k+1)/2}\|u\|_{\mathcal{C}^1(\overline{\mathsf{J}};H^{k+1,2}_{\boldsymbol{\delta}}(\Omega))}\,.$$

This shows (4.9) and completes the proof of Theorem 4.3.

6. Numerical Experiments

In this section, we conduct some numerical experiments for the piecewise linear ($p = 1$) and the piecewise quadratic ($p = 2$) SIPDG methods on graded meshes and bisection refinement meshes. The value of the penalty parameter j is chosen in a standard way as $\mathsf{j} = 10p^2$. Our main goal is to confirm the theoretical error estimates in Theorem 4.3.

6.1. **The setting.** We first detail the set-up of our experiments.

Domains. We consider the wave equation (2.4)–(2.8) with constant $\mathsf{c} = 1$. The physical domain Ω is one of the two polygons displayed in Figure 1: Both are situated in the square $(-1,1)^2$ and have the origin $\mathbf{c}_1 := (0,0)$ as sole re-entrant corner. The interior opening angle at $\mathbf{c}_i$ is selected either as $\omega_1 = 1.5\pi$ or as $\omega_1 = 1.9\pi$. Homogeneous Dirichlet boundary conditions are imposed on the edges $\{(x,y) \in$

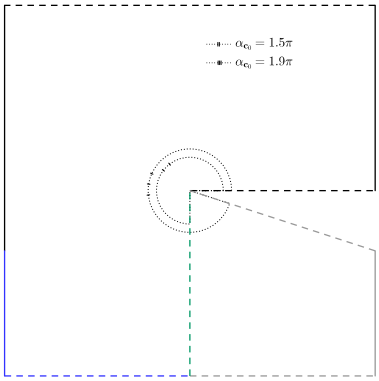

FIGURE 1. The domains Ω used in the experiments with re-entrant corner $\mathbf{c}_1 = (0,0)$ and opening angle $\omega_1 \in \{1.5, 1.9\}\pi$.

.

$\partial\Omega : x = \pm 1\}$, and homogeneous Neumann conditions on all other edges.

At the re-entrant corner $\mathbf{c}_1$, the exponent λ_1 in (2.26) satisfies $\lambda_1 \in \{2/3, 10/19\}$. Hence, in (2.20), we have

$$\delta_1^* = \max\{0, 1-\lambda_1\} = \begin{cases} 1/3 & \text{if } \omega_1 = 1.5\pi\,, \\ 9/19 & \text{if } \omega_1 = 1.9\pi\,, \end{cases} \tag{6.1}$$

where $9/19 \in (0.473, .474)$.

Initial data and right-hand side. In the following, we denote by χ_A the characteristic function of a set $A \subset \mathbb{R}^d$. Then, let $\psi_0(x) := \chi_{(-1,1)}(x)\exp(-(1-x^2)^{-1})$. This function is an element of $\mathcal{C}_0^\infty(\mathbb{R})$ with compact support in $[-1,1]$. For any $x_0 \in \mathbb{R}$ and $\varepsilon > 0$, we denote by $\phi_{x_0,\varepsilon}$ the affine equivalence from $[x_0-\varepsilon, x_0+\varepsilon]$ to $[-1,1]$. We set $\psi_{x_0,\varepsilon} := \psi_0 \circ \phi_{x_0,\varepsilon}$, which is in $\mathcal{C}_0^\infty(\mathbb{R})$ with compact support in $[x_0-\varepsilon, x_0+\varepsilon]$.

In the experiments, we now take $f \equiv 0$, $u^1 \equiv 0$. As initial condition u^0, we select

$$u^0(x,y) := \chi_{\{(x,y):x\geq 0\}}(x,y)\psi_{0.2,0.1}(x)\,. \tag{6.2}$$

That is, the initial displacement u^0 is smooth, homogeneous in y-direction and diffracts over the re-entrant corner $\mathbf{c}_1 = (0,0)$. The function u^0 satisfies the homogeneous Dirichlet conditions on Γ_D (i.e., $u^0 \in V$), but does not have compact support in Ω. Strictly speaking, the hypotheses of Proposition 2.2 are not satisfied by this initial data. On the other hand, we expect the regularity results in [28, Section 2] to hold for wider classes of compatible $\mathcal{C}^\infty$-data. This conjecture is in fact numerically corroborated for the data here.

Discretization in time. To obtain fully discrete approximations, the space semi-discrete scheme (3.8) is time-discretized with a Newmark time-stepping scheme; cf. [32, Chpt. 8] or [13, Sect. 5.1]. To this end, we introduce an equidistant partition of J given by $0 = t_0 < \Delta t < \cdots < \mathsf{N}\Delta t = \mathsf{T}$, with the time-step $\Delta t := \mathsf{T}/\mathsf{N}$. We denote by $\{u^{(n)}\}_{n=0}^{\mathsf{N}}$ the fully discrete approximations $u^{(n)} \simeq u_N(t_n) \in V_p(\mathcal{T})$. We also write $f^{(n)} := f(\cdot, t_n)$. For $\varrho \in [0, 1/2]$, $v \in V_p(\mathcal{T})$, the approximations $\{u^{(n)}\}_{n=0}^{\mathsf{N}}$ are determined by:

$$u^{(0)} := \Pi_p u^0 \,, \tag{6.3}$$

$$\Delta t^{-2}(u^{(1)} - u^{(0)} - \Delta t \Pi_p u^1, v) + \tag{6.4}$$

$$a_{DG}(\varrho(u^{(1)} - u^{(0)}) + u^0/2, v) = (\varrho f^{(1)} + (1/2 - \varrho) f^{(0)}, v) \,,$$

$$(D_2[u^{(n)}], v) + a_{DG}(\Xi_{2,\varrho}[u^{(n)}], v) = (\Xi_{2,\varrho}[f^{(n)}], v) \,, \tag{6.5}$$

where, for a generic sequence $\{w^{(n)}\}_{n=0}^{\mathsf{N}}$,

$$D_2[w^{(n)}] := \Delta t^{-2} \left(w^{(n+1)} - 2w^{(n)} + w^{(n-1)} \right) \,, \tag{6.6}$$

$$\Xi_{2,\varrho}[w^{(n)}] := \varrho w^{(n+1)} + (1 - 2\varrho) w^{(n)} + \varrho w^{(n-1)}. \tag{6.7}$$

We remark that the iteration (6.3)–(6.5) coincides with the standard two-parameter Newmark scheme as in e.g. [32, Chpt. 8], with fixed value $\gamma = 1/2$ for the second parameter γ in the notation of [32]. It is then second-order accurate in the time-step Δt.

For $\varrho = 0$, the time-stepping (6.3)–(6.5) amounts to solving for a (block-diagonal) DG mass-matrix in each time-step and thus leads essentially to an explicit scheme. One the other hand, $\varrho > 0$ gives rise to an implicit method which is conditionally stable for $0 \leq \varrho < 1/4$ and unconditionally stable for $\varrho \geq 1/4$; cf. [32, Lem. 8.5.1].

To confirm the spatial error bounds in Theorem 4.3 numerically, we take $\mathsf{T} = 1$ and discretize (3.8) in time by using the Newmark method (6.3)–(6.5) with $\varrho = 1/4$ and time-step $\Delta t = 10^{-4}$. This time-step is sufficiently small in relation to the spatial dimension N and thus ensures that the approximation errors stemming from the time-discretization are negligible with respect to the space discretization errors.

Error computation and reference solution. In our error computations, we compare the numerical solutions $\{u^{(n)}\}_{n=0}^{\mathsf{N}}$ to a reference solution $\{u_{ref}^{(n)}\}_{n=0}^{2\mathsf{N}}$, which is obtained by the same algorithm, but for a reference mesh where two additional refinements are performed on the finest grid used and for a time partition with time-step $\Delta t/2$. We then compute the errors

$$\max_{n=0}^{\mathsf{N}} \|u^{(n)} - u_{ref}^{(2n)}\|, \tag{6.8}$$

for $\|\cdot\| = |\!|\!| \cdot |\!|\!|_{DG}$ and $\|\cdot\| = \|\cdot\|_{\mathcal{L}^2(\Omega)}$, which are discrete versions of the norms $\|\cdot\|_{\mathcal{L}^\infty(\mathsf{J};\mathcal{V}_p(\mathcal{T}))}$ and $\|\cdot\|_{\mathcal{L}^\infty(\mathsf{J};\mathcal{L}^2(\Omega))}$ appearing in (4.8) and (4.9), respectively.

We visualize the relative errors thus obtained on a bi-logarithmic scale with $\#\mathcal{T} \simeq N$ on the abscissa and the error on the ordinate axis. In this scale, the convergence order $\mathcal{O}(N^{-r})$ with respect to N is represented by a line of slope $-r$. Conversely, a line of slope $-r$ is said to be convergent of order r. The convergence order of the line fitted through the data points in the least-squares sense is called the *empirical convergence order*.

Specifications of the code. The code used in our tests is written in Python 2.7 and depends on the libraries NumPy 1.10.1 and SciPy 0.16.1; see [17]. The resulting linear systems of equations are solved using the direct solver `spsolve` included in the SciPy submodule `scipy.sparse.linalg`.

Local mesh refinement. Graded meshes are generated using the free software package `LNG_FEM`; see [22]. To generate meshes with local bisection refinement, we first create regular and quasi-uniform triangulation $\mathcal{T}_0$ of Ω with mesh-width $h(\mathcal{T}_0) = 0.1$, using the Delaunay-based mesh generator contained in the Python library `triangle`; see [36]. Then the local bisection refinement algorithm in [11] with parameters h, γ and L is applied. Elements are bisected according to newest vertex bisection; see, e.g. [29] and the references therein for a specification. Note also that the elementary bisection of elements needs to include a recursive call in order to ensure the output of regular triangulations without hanging nodes. In order to fulfill the second condition in (4.2), we choose L in dependence of h and γ as

$$L = \lceil -\frac{\log_2(h)}{\gamma(p+1)} - 1 \rceil. \tag{6.9}$$

The refinement parameters for locally refined meshes in Definition 4.2 are taken with respect to δ_1^* in (6.1). That is, for graded meshes, we choose the grading parameter $\beta_1 = \beta_1^* = 1 - \frac{1-\delta_1^*}{p}$ as in (4.1); for bisection refinement meshes, we select $\gamma = \gamma^* = 1 - \delta_1^*$ in (4.2). Since bisection refinement meshes are nested with respect to L in (6.9), the reference solution can be straightforwardly projected onto coarser grids for error computations.

6.2. **Results.** We next present the numerical results obtained in the set-up described in Section 6.1.

6.2.1. *Piecewise linear SIPDG method.* We first consider $p = 1$, $\mathrm{j} = 10$ and depict the results obtained in this way in Figure 2. The relative errors to the reference solution are evaluated as in (6.8), i.e., in (the approximate versions of) the norms $\|\cdot\|_{\mathcal{L}^\infty(\mathsf{J};\mathcal{V}_p(\mathcal{T}))}$ (labelled "DG norm") and $\|\cdot\|_{\mathcal{L}^\infty(\mathsf{J};\mathcal{L}^2(\Omega))}$ (labelled "$\mathcal{L}^2$ norm"), respectively. We also display the lines of convergence orders $r = 0.5$ and $r = 1.0$, respectively.

The empirical convergence rates for both graded and bisection refinement meshes are of the orders $r = 0.5$ and $r = 1.0$ for the DG energy norm errors predicted by our theory. The $\mathcal{L}^2$-norm errors, respectively, are also in accordance with Theorem 4.3. As expected, the empirical convergence rate does not change with the interior opening angle ω_1, while the number of degrees of freedom naturally does.

6.2.2. *Piecewise quadratic SIPDG method.* Next, we consider the piecewise quadratic ($p = 2$) SIPDG discretization with $\mathrm{j} = 40$, and plot the corresponding results in Figure 3.

Again, the empirical convergence rates both for graded and bisection refinement meshes are of the expected orders $r = 1.0$ and $r = 1.5$ in the DG energy norm errors and the $\mathcal{L}^2$-norm errors, respectively, thereby confirming Theorem 4.3 also for this example. As before, these rates are quasi-optimal and do not change with the interior opening angle ω_1.

We remark that in comparison to the meshes in the piecewise linear case, the *number* of elements remains the same for graded meshes. However, the elemental

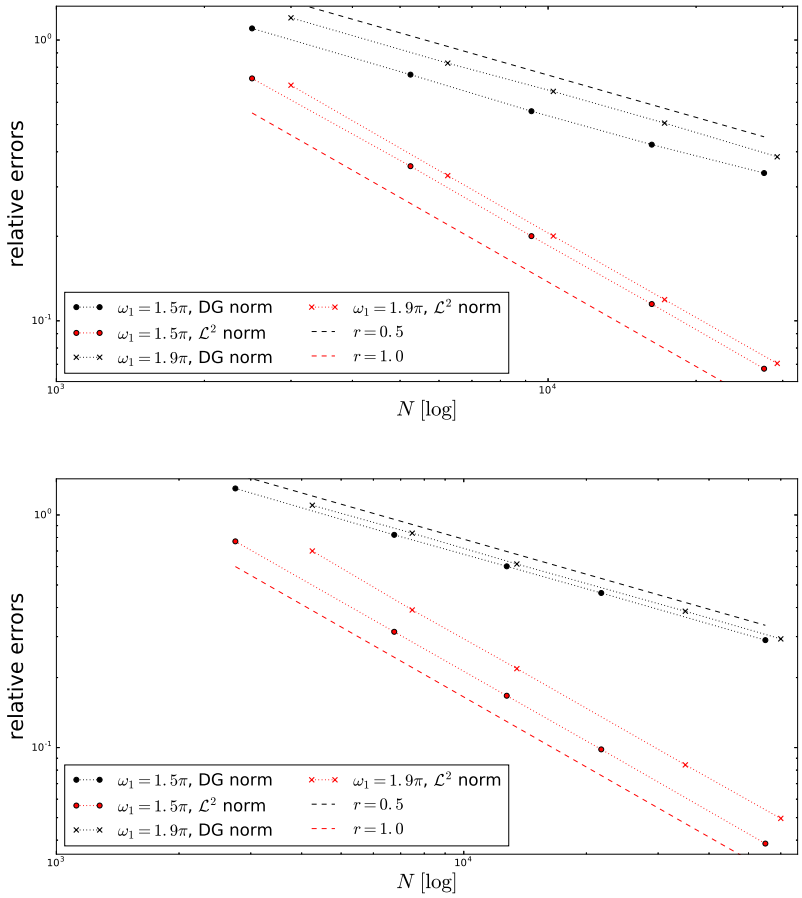

FIGURE 2. Convergence plots for piecewise linear ($p = 1$) SIPDG discretization with $\mathsf{j} = 10$. Top: graded meshes with grading parameter β_1^*. Bottom: bisection refinement meshes with weight $\gamma^* = 1 - \delta_1^*$.

mesh sizes now decrease faster at the vertex $\mathbf{c}_1$ since the grading is now stronger according to (4.1). For meshes with local bisection refinement, it is not necessary to construct the mesh anew, but the number L of local refinements increases according to (4.2) and (6.9).

7. Conclusions and Extensions

We proved that SIPDG discretizations in space of the wave equation converges in a space semi-discrete sense with optimal convergence rates, both in the DG energy norm and the $\mathcal{L}^2$ norm (where we use the generalized Aubin-Nitsche argument from [25, Sect. 5.4.2] for the Galerkin projection). We note that these convergence rates are lost on quasi-uniform mesh families due to the appearance of singularities

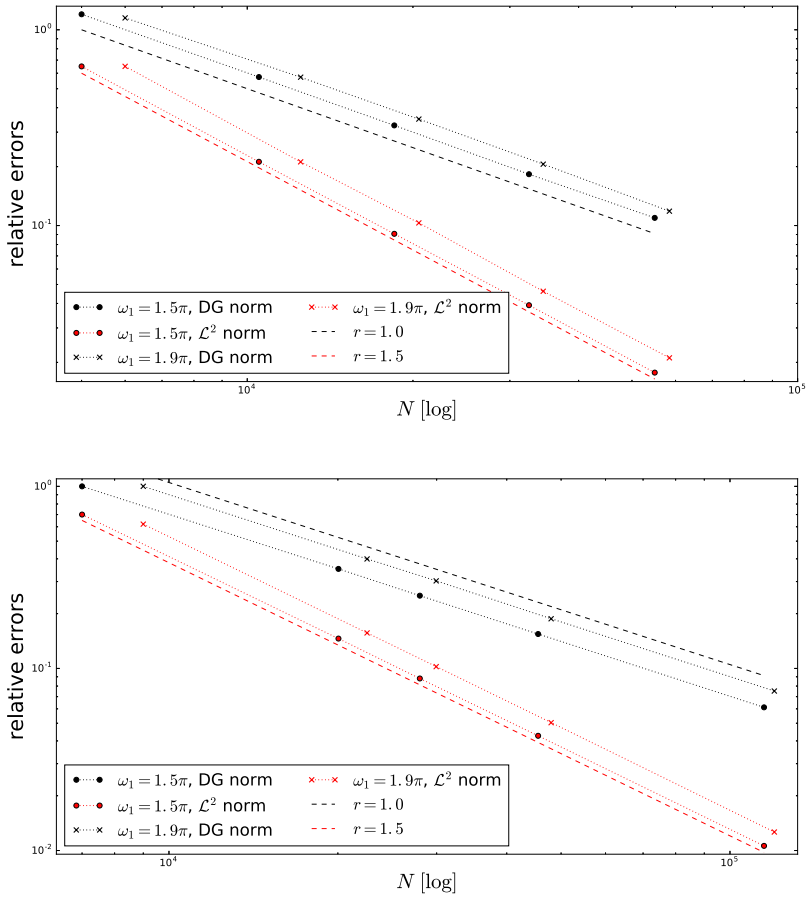

FIGURE 3. Convergence plots for piecewise quadratic ($p = 2$) SIPDG discretization with $\mathsf{j} = 40$. Top: graded meshes with grading parameter β_1^*. Bottom: bisection refinement meshes with weight $\gamma^* = 1 - \delta_1^*$.

near corners. Our results are based on employing either graded meshes with appropriate grading parameters or local mesh refinement towards the corners by newest vertex bisection. The theoretical convergence orders are confirmed in a series of numerical tests.

For simplicity, our analysis was carried out for regular meshes. However, with only minor modifications, it can be extended to simplicial mesh families with k-irregular nodes, which are a particular case of the shape-regular and contact-regular mesh families introduced in [30, Sect. 1.4].

For simplicity, we focussed on constant wave speed coefficients c, but emphasize that our results can be readily generalized to transmission problems with piecewise constant coefficient c. In particular, the regularity results in Proposition 2.2 hold true for this case as well; see [28, Section 2.6.2].

References

1. J. Adler and V. Nistor, *Graded mesh approximation in weighted Sobolev spaces and elliptic equations in 2D*, Math. Comp. **84** (2015), no. 295, 2191–2220. MR 3356024
2. D. Arnold, F. Brezzi, B. Cockburn, and D. Marini, *Unified analysis of discontinuous Galerkin methods for elliptic problems*, SIAM J. Numer. Anal. **39** (2002), no. 5, 1749–1779. MR 1885715 (2002k:65183)
3. I. Babuška and B. Q. Guo, *The h-p version of the finite element method for domains with curved boundaries*, SIAM J. Numer. Anal. **25** (1988), no. 4, 837–861. MR 954788
4. ———, *Regularity of the solution of elliptic problems with piecewise analytic data. I. Boundary value problems for linear elliptic equation of second order*, SIAM J. Math. Anal. **19** (1988), no. 1, 172–203. MR 924554
5. I. Babuška, R.B. Kellogg, and J. Pitkäranta, *Direct and inverse error estimates for finite elements with mesh refinements*, Numer. Math. **33** (1979), no. 4, 447–471. MR 553353 (81c:65054)
6. C. Băcuţă, H. Li, and V. Nistor, *Differential operators on domains with conical points: precise uniform regularity estimates*, arXiv preprint (2016), no. 1605.07907.
7. C. Băcuţă, V. Nistor, and L.T. Zikatanov, *Improving the rate of convergence of 'high order finite elements' on polygons and domains with cusps*, Numer. Math. **100** (2005), no. 2, 165–184. MR 2135780 (2006d:65130)
8. G. Cohen, P. Joly, and N. Tordjman, *Construction and analysis of higher order finite elements with mass lumping for the wave equation*, Second International Conference on Mathematical and Numerical Aspects of Wave Propagation (Newark, DE, 1993), SIAM, Philadelphia, PA, 1993, pp. 152–160. MR 1227833 (94d:65058)
9. R. Dautray and J.-L. Lions, *Mathematical analysis and numerical methods for science and technology. Vol. 5*, Springer-Verlag, Berlin, 1992, Evolution problems. I, With the collaboration of Michel Artola, Michel Cessenat and Hélène Lanchon, Translated from the French by Alan Craig. MR 1156075 (92k:00006)
10. A. Ern and J.-L. Guermond, *Theory and practice of finite elements*, Applied Mathematical Sciences, vol. 159, Springer, 2004.
11. F.D. Gaspoz and P. Morin, *Convergence rates for adaptive finite elements*, IMA J. Numer. Anal. **29** (2009), no. 4, 917–936. MR 2557050 (2010k:65257)
12. P. Grisvard, *Elliptic problems in nonsmooth domains*, Monographs and Studies in Mathematics, vol. 24, Pitman, Boston, 1985.
13. M. Grote, A. Schneebeli, and D. Schötzau, *Discontinuous Galerkin finite element method for the wave equation*, SIAM J. Numer. Anal. **44** (2006), no. 6, 2408–2431. MR 2272600 (2007k:65149)
14. M. Grote and D. Schötzau, *Optimal error estimates for the fully discrete interior penalty DG method for the wave equation*, J. Sci. Comput. **40** (2009), 257–272.
15. B. Q. Guo and I. Babuška, *The hp-version of the finite element method. Part I: The basic approximation results*, Comp. Mech. **1** (1986), 21–41.
16. M. Hochbruck and A. Sturm, *Error analysis of a second-order locally implicit method for linear Maxwell's equations*, SIAM J. Numer. Anal. **54** (2016), no. 5, 3167–3191. MR 3565552
17. E. Jones, T. Oliphant, P. Peterson, et al., *SciPy: Open Source Scientific Tools for Python*, 2017.
18. U. Köcher and M. Bause, *Variational space-time methods for the wave equation*, J. Sci. Comput. **61** (2014), no. 2, 424–453. MR 3265256
19. A. Yu. Kokotov and B. A. Plamenevskiĭ, *On the asymptotic behavior of solutions of the Neumann problem for hyperbolic systems in domains with conical points*, Algebra i Analiz **16** (2004), no. 3, 56–98. MR 2083566
20. V. A. Kondrat'ev, *Boundary value problems for elliptic equations in domains with conical or angular points*, Trudy Moskov. Mat. Obšč. (1967).
21. V. A. Kozlov, V. G. Mazya, and J. Rossmann, *Spectral problems associated with corner singularities of solutions to elliptic equations*, Mathematical Surveys and Monographs, vol. 85, American Mathematical Society, Providence, RI, 2001. MR 1788991 (2001i:35069)
22. H. Li and V. Nistor, *LNG– FEM: graded meshes on domains of polygonal structures*, Recent Advances in Scientific Computing and Applications, Contemp. Math., vol. 586, Amer. Math. Soc., Providence, RI, 2013, pp. 239–246. MR 3075874

23. S. I. Matyukevich and B. A. Plamenevskiĭ, *On dynamic problems in the theory of elasticity in domains with edges*, Algebra i Analiz **18** (2006), no. 3, 158–233. MR 2255852
24. V. Maz'ya and J. Rossmann, *Elliptic equations in polyhedral domains*, Mathematical Surveys and Monographs, vol. 162, American Mathematical Society, Providence, RI, 2010. MR 2641539 (2011h:35002)
25. F. Müller, D. Schötzau, and Ch. Schwab, *Symmetric interior penalty discontinuous Galerkin methods for elliptic problems in polygons*, Tech. Report 2017–15, Seminar for Applied Mathematics, ETH Zürich, Zürich, Switzerland, 2017, (in press in SIAM J. Num. Analysis (2018)).
26. F. Müller and Ch. Schwab, *Finite elements with mesh refinement for wave equations in polygons*, J. Comput. Appl. Math. **283** (2015), 163–181. MR 3317277
27. F. Müller and Ch. Schwab, *Finite elements with mesh refinement for elastic wave propagation in polygons*, Math. Meth. Appl. Sci. **39** (2016), 5027–5042.
28. Fabian Müller, *Numerical analysis of finite element methods for second order wave equations in polygons*, Ph.D. thesis, ETH Zürich, 2017, Diss. ETH No. 24385.
29. R.H. Nochetto, K.G. Siebert, and A. Veeser, *Theory of adaptive finite element methods: an introduction*, Multiscale, Nonlinear and Adaptive Approximation, Springer, Berlin, 2009, pp. 409–542. MR 2648380 (2011k:65164)
30. D.A. Di Pietro and A. Ern, *Mathematical aspects of discontinuous Galerkin methods*, Mathématiques & Applications (Berlin) [Mathematics & Applications], vol. 69, Springer, Heidelberg, 2012. MR 2882148
31. B. A. Plamenevskiĭ, *On the wave equation in a cylinder with edges*, Funktsional. Anal. i Prilozhen. **32** (1998), no. 1, 81–84. MR 1627239 (99b:35113)
32. P.-A. Raviart and J.-M. Thomas, *Introduction à l'analyse numérique des equations aux derivées partielles*, Dunod, Paris, 1998, in French.
33. B. Rivière, *Discontinuous galerkin methods for solving elliptic and parabolic problems: Theory and implementation*, Frontiers in Applied Mathematics, SIAM, 2008.
34. D. Schötzau and Ch. Schwab, *Exponential convergence of hp-FEM for elliptic problems in polyhedra: Mixed boundary conditions and anisotropic polynomial degrees*, Found. Comput. Math. (2017).
35. Ch. Schwab, *p- and hp-FEM – Theory and application to solid and fluid mechanics*, Oxford University Press, Oxford, 1998.
36. J. R. Shewchuk, *Triangle: Engineering a 2D quality mesh generator and Delaunay triangulator*, Applied Computational Geometry: Towards Geometric Engineering (M. C. Lin and D. Manocha, eds.), Lecture Notes in Computer Science, vol. 1148, Springer Verlag, 1996, pp. 203–222.
37. T. P. Wihler, *Discontinuous Galerkin FEM for Elliptic Problems in Polygonal Domains*, Ph.D. thesis, Swiss Federal Institute of Technology Zurich, 2002, Diss. ETH No. 14973.
38. J. Wloka, *Partielle Differentialgleichungen: Sobolevräume und Randwertaufgaben*, Mathematische Leitfäden, B. G. Teubner, Stuttgart, 1982, in German. MR 652934 (84a:35002)

Seminar for Applied Mathematics, ETH Zürich, Rämistrasse 101, 8092 Zürich, Switzerland.

E-mail address: muelfabi@ethz.ch

Mathematics Department, University of British Columbia, 1984 Mathematics Road, Vancouver, BC, V6T 1Z2, Canada.

E-mail address: schoetzau@math.ubc.ca

Seminar for Applied Mathematics, ETH Zürich, Rämistrasse 101, 8092 Zürich, Switzerland.

E-mail address: schwab@math.ethz.ch